

Non-perturbative evaluation for anomalous dimension in 2-dimensional $O(3)$ sigma model

Sergio Calle Jimenez,¹ Makoto Oka,^{1,2} and Kiyoshi Sasaki¹

¹ *Department of Physics, Tokyo Institute of Technology, Tokyo 152-8551, Japan*

² *Advanced Science Research Center,*

Japan Atomic Energy Agency, Tokai, Ibaraki 319-1195, Japan

Abstract

We calculate the wave-function renormalization in 2-dimensional $O(3)$ sigma model, non-perturbatively. It is evaluated in a box with a finite spatial extent. We determine the anomalous dimension in the finite volume scheme through an analysis of the step scaling function. Results are compared with a perturbative evaluation, and the reasonable behavior is confirmed.

PACS numbers: 11.10.Hi, 11.10.Kk, 11.10.Lm, 11.15.Ha

I. INTRODUCTION

In the late '80s and the early '90s, some people have developed methods to extract information at infinite volume from the information on a system in a finite box. One is to calculate the scattering phase shift [1], and another is to determine the running coupling constant [2]. The latter prescribes a renormalization group (RG) evolution of the renormalized coupling as a response to change of the box size. The workability of this method might give us a foresight of the existence of RG equation which describes the box-size dependence of N -point Green function. It will be useful to describe a spatially extended object in a finite box. An example is the deuteron, and another one is the Efimov system [3]. For the latter, the infinity of the object size is essential, so that we cannot avoid a discussion of the box-size dependence in a study with a lattice simulation.

The end goal of our study is to establish such a RG equation. For this purpose, we use the 2-dimensional $O(n)$ sigma model. Until now, however, the wave-function renormalization has not been discussed in the context where the system has been put in a finite box. For the establishment of the RG equation, one might need information on the scale dependence of wave-function renormalization, which is called anomalous dimension. The present work aims to give a non-perturbative evaluation for the anomalous dimension as a first step for constructing the RG equation.

Before entering the main issue, we summarize the basic properties on the 2-dimensional $O(n)$ sigma model [4] from the standpoint of perturbative studies. In the middle '70s, the renormalizability, and the asymptotic freedom have been established [5, 6]. The asymptotic freedom is important to guarantee the applicability of the perturbative expansion in the high-energy region. Then, the renormalization above 2 dimension has been also discussed [7, 8]. The infrared (IR) divergence is regularized with a magnetic field in these studies. A vanishment of the magnetic field activates the IR divergence, again. However, the renormalization in minimal subtraction (MS) scheme [9] requires only the cancellation of ultraviolet (UV) divergence. If we restrict ourselves to evaluate the renormalization factor, the IR divergence is not a difficulty. On the other hands, if we focus on a physical quantity like a mass gap, the IR divergence is a serious problem.

The IR divergence originates from the low dimensionality of the system. Mermin-Wagner's theorem forbids spontaneous symmetry breaking in 2 dimension [10]. The perturbative expansion with a fixed direction of the magnetization cannot be justified. As the results, the IR divergence remains in the the Green function of the pion mode. It has been conjectured by Elitzur [11] and proved by David [12] that the $O(n)$ -invariant Green function including the sigma mode is IR finite. Then, the $O(n)$ -invariant Green function in a finite box has been discussed, and the value of the mass gap has been evaluated [2, 13–16]. In these studies, the particular attention is payed for the treatment of the zero mode. There are several methods. One is to add compact extra dimensions [13]. Another is to separate the collective motion of the magnetization [14]. Another is to use a background field [15, 16]. The other is to introduce the IR-cutoff mass by using the lattice regularization [2]. We add that some works are relatively recently performed besides these works [17–20].

At present, we have no difficulty to evaluate the mass gap of the 2-dimensional $O(n)$ sigma model in a finite box regardless of perturbatively or non-perturbatively. The mass gap can be used to define the renormalized coupling, and discuss the scale dependence of it [2]. On the other hands, having the $O(n)$ -invariant 2-point Green function, it is also easy to evaluate the amplitude. Then, we can define the wave-function renormalization from the amplitude, and discuss the scale dependence. This is just the theme addressed in the present study.

This article is organized as follows. In Sec. II, we introduce the 2-dimensional $O(n)$ sigma model. Then, we briefly describe a renormalization in the finite volume scheme and the procedure to determine the evolution of parameters of the theory. In Sec. III, the details of Monte Carlo simulation are explained. In Sec. IV, we show the results for the wave-function renormalization in addition to results for the renormalized coupling. We also discuss their scale dependence. In Sec. V, our conclusions are given.

II. MODEL, RENORMALIZATION SCHEME AND SCALE DEPENDENCE

A. 2-dimensional $O(n)$ sigma model

The 2-dimensional $O(n)$ sigma model is formally prescribed by the euclidean action

$$S[\phi] = \frac{1}{2g^2} \int d^2x \partial_\mu \phi(x) \cdot \partial_\mu \phi(x) \quad (\mu = 0, 1) . \quad (1)$$

Here $\phi(x) = (\phi_i(x), i = 1, \dots, n)$ is the n -component field with the constraint

$$\phi(x) \cdot \phi(x) = 1 . \quad (2)$$

The bullet point symbol denotes the scalar product of n -component vectors. The system is put on a finite box with the temporal extent T and the spatial extent L . We assume that T is sufficiently large compared to L . In the present work, we impose the Neumann boundary condition (NBC) for the temporal direction, and the periodic boundary condition (PBC) for the spatial direction,

$$\frac{\partial}{\partial x_0} \phi(x_0, x_1) = 0 \quad (x_0 \in \partial\Lambda_\tau) , \quad \phi(x_0, x_1 + Ln) = \phi(x_0, x_1) \quad (n \in \mathbb{Z}) , \quad (3)$$

where $\partial\Lambda_\tau$ represents the temporal boundary. The reason why we use the NBC in the temporal direction is to realize the $O(n)$ -invariant state at $\partial\Lambda_\tau$. As the results, states other than the spin-1 state do not contribute the 2-point Green function. The NBC is called also the free boundary condition.

As we have said in Sec. I, the $O(n)$ -invariant Green function should be used to avoid the IR divergence. The $O(n)$ -invariant 2-point Green function is defined by

$$G_{\text{inv}}(x; y) = \langle \phi(x) \cdot \phi(y) \rangle , \quad (4)$$

where the angle bracket refers to the expectation values over the configurations of ϕ field. We consider the zero-momentum projected Green function,

$$G_{\text{inv}}(x_0; y_0) = \frac{1}{L^2} \int dx_1 dy_1 e^{-ip_1(y_1-x_1)} G_{\text{inv}}(x; y) \Big|_{p_1=0} . \quad (5)$$

With the NBC for the temporal direction, it can be written as

$$G_{\text{inv}}(x_0; y_0) = A e^{-M|y_0-x_0|} + \mathcal{O}(e^{-(4\pi/L)|y_0-x_0|}) . \quad (6)$$

For our purpose, the mass gap M and the amplitude A are needed. Energies of the excited states are known to be at least $4\pi/L$. With a finite L , they are large enough to ignore the contributions to $G_{\text{inv}}(x_0; y_0)$.

B. Renormalization scheme

The renormalization of the 2-dimensional $O(n)$ sigma model is done by the replacement

$$g^2 = Z_{\text{R}}^g g_{\text{R}}^2 , \quad (7)$$

$$\phi(z) = (Z_{\text{R}}^\phi)^{1/2} \phi_{\text{R}}(z) . \quad (8)$$

Here g_{R}^2 is the renormalized coupling, and $\phi_{\text{R}}(z)$ is the renormalized field. We have a finite arbitrariness for the choice of them. This arbitrariness can be removed by setting values of g_{R}^2 and the wave-function renormalization Z_{R}^ϕ at an energy scale μ . Such conditions are called renormalization conditions. The definition of μ in the MS scheme is given in Sec. A.

In the present study, we consider the renormalization conditions at $\mu = 1/L$ as

$$\frac{n-1}{2L} g_{\text{FV}}^2(\mu) \Big|_{\mu=1/L} = M , \quad (9)$$

$$Z_{\text{FV}}^\phi(\mu) \Big|_{\mu=1/L} = A . \quad (10)$$

M and A are the mass gap and amplitude, respectively, which are determined from the measured value of the $O(n)$ -invariant 2-point Green function. The renormalized coupling in Eq. (9) has been first proposed in Ref. [2], and called the finite volume (FV) coupling. In the following, we refer Eqs. (9) and (10) by renormalization in the FV scheme. As long as there is no confusion, we write the argument of g_{FV}^2 and Z_{FV}^ϕ by L , but not $1/L$.

The β function and the anomalous dimension describe μ dependence of the renormalized parameters with the fixed bare parameters g^2 and $\phi(x)$. They are defined as

$$\beta_{\text{R}}(g_{\text{R}}^2) \equiv \mu \frac{d}{d\mu} g_{\text{R}}^2(\mu) , \quad (11)$$

$$\gamma_{\text{R}}(g_{\text{R}}^2) \equiv \mu \frac{d}{d\mu} \ln Z_{\text{R}}^\phi(\mu) , \quad (12)$$

respectively. In the FV scheme, they are written as

$$\beta_{\text{FV}}(g_{\text{FV}}^2) = -L \frac{d}{dL} g_{\text{FV}}^2(L) , \quad (13)$$

$$\gamma_{\text{FV}}(g_{\text{FV}}^2) = -L \frac{d}{dL} \ln Z_{\text{FV}}^\phi(L) , \quad (14)$$

by using $\mu = 1/L$ to Eqs. (11) and (12).

C. Scale dependence

The step scaling function (SSF) describes how parameters of a theory evolves when the scale is changed. We consider two types of SSFs, σ^g and σ^ϕ . They are defined through

$$g_{\text{FV}}^2(sL) = \sigma^g(s, g_{\text{FV}}^2(L)) , \quad (15)$$

$$Z_{\text{FV}}^\phi(sL) = \sigma^\phi(s, g_{\text{FV}}^2(L)) Z_{\text{FV}}^\phi(L) , \quad (16)$$

with a scaling factor s . $\sigma^g(s, g_{\text{FV}}^2)$ is proposed in Ref. [2], and $\sigma^\phi(s, g_{\text{FV}}^2)$ is motivated from Ref. [21]. They are related to $\beta_{\text{FV}}(g_{\text{FV}}^2)$ and $\gamma_{\text{FV}}(g_{\text{FV}}^2)$ by

$$\beta_{\text{FV}}(\sigma^g(s, g_{\text{FV}}^2)) = -s \frac{\partial \sigma^g(s, g_{\text{FV}}^2)}{\partial s} , \quad (17)$$

$$\gamma_{\text{FV}}(\sigma^g(s, g_{\text{FV}}^2)) = -s \frac{\partial \ln \sigma^\phi(s, g_{\text{FV}}^2)}{\partial s} , \quad (18)$$

respectively. However, the SSFs are directly related with values measured in a Monte Carlo simulation in contrast to $\beta_{\text{FV}}(g_{\text{FV}}^2)$ and $\gamma_{\text{FV}}(g_{\text{FV}}^2)$.

If $\beta_{\text{FV}}(g_{\text{FV}}^2)$ and $\gamma_{\text{FV}}(g_{\text{FV}}^2)$ are perturbatively known, $\sigma^g(s, g_{\text{FV}}^2)$ and $\sigma^\phi(s, g_{\text{FV}}^2)$ can be evaluated. Using an abbreviation $u \equiv g_{\text{FV}}^2$ to simplify the expression, we consider the perturbative expansions of $\beta_{\text{FV}}(u)$ and $\gamma_{\text{FV}}(u)$

$$\beta_{\text{FV}}(u) = -u^2 \sum_{i=0}^{\infty} \beta_{\text{FV},i} u^i , \quad \gamma_{\text{FV}}(u) = -u \sum_{i=0}^{\infty} \gamma_{\text{FV},i} u^i , \quad (19)$$

and ones of the SSFs

$$\sigma^g(s, u) = u + u \sum_{i=0}^{\infty} \sigma_i^g(s) u^{i+1} , \quad \sigma^\phi(s, u) = 1 + \sum_{i=0}^{\infty} \sigma_i^\phi(s) u^{i+1} . \quad (20)$$

By substituting Eqs. (19) and (20) to Eqs. (17) and (18), and by comparing the coefficients at the same order of u , we obtain

$$\begin{aligned} \sigma_0^g(s) &= \beta_{\text{FV},0} \ln s , & \sigma_1^g(s) &= \beta_{\text{FV},1} \ln s + \beta_{\text{FV},0}^2 (\ln s)^2 , \\ \sigma_2^g(s) &= \beta_{\text{FV},2} \ln s + \frac{5}{2} \beta_{\text{FV},0} \beta_{\text{FV},1} (\ln s)^2 + \beta_{\text{FV},0}^3 (\ln s)^3 , \end{aligned} \quad (21)$$

and

$$\begin{aligned} \sigma_0^\phi(s) &= \gamma_{\text{FV},0} \ln s , & \sigma_1^\phi(s) &= \gamma_{\text{FV},1} \ln s + \frac{1}{2} (\beta_{\text{FV},0} + \gamma_{\text{FV},0}) \gamma_{\text{FV},0} (\ln s)^2 , \\ \sigma_2^\phi(s) &= \gamma_{\text{FV},2} \ln s + (\beta_{\text{FV},0} \gamma_{\text{FV},1} + \gamma_{\text{FV},0} \gamma_{\text{FV},1} + \beta_{\text{FV},1} \gamma_{\text{FV},0} / 2) (\ln s)^2 \\ &\quad + \frac{1}{3} (\beta_{\text{FV},0} + \gamma_{\text{FV},0}) (\beta_{\text{FV},0} + \gamma_{\text{FV},0} / 2) \gamma_{\text{FV},0} (\ln s)^3 , \end{aligned} \quad (22)$$

up to the 3-loop order. Note that all the coefficients in $\sigma_i^g(s)$ and $\sigma_i^\phi(s)$ are not independent due to the constraint $\sigma^{g,\phi}(s_2 s_1, u) = \sigma^{g,\phi}(s_2, \sigma^g(s_1, u))$.

Later, we need the perturbative evaluation of $\sigma^{g,\phi}(s, u)$. They are evaluated by Eq. (20) with Eqs. (21) and (22) obtained from

$$\begin{aligned}\beta_{\text{FV},0} &= \frac{n-2}{2\pi}, & \beta_{\text{FV},1} &= \frac{n-2}{4\pi^2}, & \beta_{\text{FV},2} &= \frac{(n-1)(n-2)}{8\pi^3}, \\ \gamma_{\text{FV},0} &= -\frac{n-1}{2\pi}, & \gamma_{\text{FV},1} &= 0, & \gamma_{\text{FV},2} &= 0,\end{aligned}\tag{23}$$

and $\sigma_i^{g,\phi}(s) = 0$ for $i \geq 3$. We refer these SSFs by $\sigma_p^{g,\phi}(s)$. The derivation of Eq. (23) is given in Sec. A.

III. DETAILS OF MONTE CARLO SIMULATION

A. Setup

We set $n = 3$. The calculation is performed on the $(T/a) \times (L/a)$ lattice with $T = 5L$. Here a is the lattice spacing, and is determined from the bare coupling g^2 . Due to the discretization, the action is changed to

$$S_{\text{lat}}[\phi] = -\frac{1}{g^2} \sum_{x,\mu} \phi(x) \cdot \phi(x + \hat{\mu}),\tag{24}$$

where x moves all the lattice space-time points, and $\hat{\mu}$ is a unit vector in the μ direction. The NBC is imposed for the temporal direction, and the PBC for the spatial direction. In Table I, we list $(1/g^2, L/a)$ which are used in the present calculation. As we will mention in Sec. IV A, we classify them into five sets (“A”, “B”, “C”, “D” and “E”) depending on the value of renormalized coupling. For updating of ϕ configurations, the heat bath algorithm is used, and even sites and odd sites are alternately updated. After the thermalization by 5000 sweeps, we calculate

$$G_{\text{inv}}^{(i)}(t) = \frac{1}{L^2} \sum_{x_1, y_1} \phi(t_{\text{src}}, x_1) \cdot \phi(t, y_1)\tag{25}$$

on the i -th configuration at every 100 sweeps. We set $t_{\text{src}}/a = L/a$. The total number of samples is 999950 for each parameter set. The expectation value of Eq. (25) is nothing less than the $O(n)$ -invariant 2-point Green function.

B. Autocorrelation

We consider the autocorrelation function of $G_{\text{inv}}^{(i)}(t)$,

$$A(j) \equiv \frac{1}{N} \sum_{i=1}^N \left[\left(G_{\text{inv}}^{(i)}(t) - \langle G_{\text{inv}}(t) \rangle_0 \right) \left(G_{\text{inv}}^{(i+j)}(t) - \langle G_{\text{inv}}(t) \rangle_j \right) \right],\tag{26}$$

where the angle bracket denotes the expectation value as

$$\langle G_{\text{inv}}(t) \rangle_j \equiv \frac{1}{N} \sum_{i=1}^N G_{\text{inv}}^{(i+j)}(t). \quad (27)$$

The function $A(j)$ represents the correlation between $G_{\text{inv}}^{(i)}(t)$'s separated by the j -time measurements. For a precise analysis, we introduce the integrated autocorrelation time,

$$\tau_{\text{int}}(j) = \frac{1}{2} + \sum_{i=1}^j \frac{A(i)}{A(0)}. \quad (28)$$

$2\tau_{\text{int}}(\infty)$ will indicate the separation where the measurements can be regarded to be independent.

In Fig. 1, we give $2\tau_{\text{int}}(j)$ for some $(1/g^2, L/a)$'s. To guarantee a reliable analysis, $N \gg j$ is required, and we adopt $N = 100000$. The statistical error is evaluated by the single-eliminated jackknife method. The autocorrelation time becomes large near the continuum limit, so that we show the data for $1/g^2$ which gives the smallest lattice spacing from the sets A and E. For each $(1/g^2, L/a)$, the situations with $(t - t_{\text{src}})/a = 10, 20$ and 30 are shown. The data with large $(t - t_{\text{src}})/a$ do not give a significant contribution for the evaluation of the mass gap and amplitude. We consider that the verification at $(t - t_{\text{src}})/a = 10 - 30$ is sufficient. We confirm, from Fig. 1, that $2\tau_{\text{int}}(\infty)$ is at most about 10 with our simulation parameters. For the sake of safety, we evaluate the statistical errors on the mass gap and amplitude by the jackknife method with the bin size of 50 samples in the following analysis.

C. Fit range

For the $O(N)$ -invariant 2-point Green function, we carry out the fit considering the correlation between the different time slices with the variance-covariance matrix. We refer the fit range by $[t_{\text{min}} : t_{\text{max}}]$. For all the parameter sets, $(t_{\text{max}} - t_{\text{src}})/a = 3(L/a) - 1$ is chosen to avoid the contamination from the temporal boundary. On the other hand, t_{min} should be determined from the behavior of χ^2/N_{df} . We increase t_{min} from 1, and adopt the value when χ^2/N_{df} falls to the vicinity of 1. An example for $(1/g^2, L/a) = (2.2403, 32)$ is shown in Fig. 2. For this parameter set, $(t_{\text{min}} - t_{\text{src}})/a = 12$ is adopted, and the fitted value is shown by the horizontal dotted lines.

IV. NUMERICAL RESULTS

A. Data of SSF

We obtain the mass gap in the lattice unit Ma and the amplitude A by fitting Eq. (6) to the data of $O(n)$ -invariant 2-point Green function. The renormalized coupling g_{FV}^2 can be extracted from Ma by Eq. (9), and the wave-function renormalization Z_{FV}^ϕ from A by

Eq. (10). On a lattice, g_{FV}^2 and Z_{FV}^ϕ depend on L/a in addition to the physical extent L . To take the continuum limit later, we classify the numerical data into five sets (“A”, “B”, “C”, “D” and “E”). The classification is based on the value of g_{FV}^2 in the smallest L for each $1/g^2$. We refer the smallest L by L_0 . In Tables II, III, IV, V and VI, we show $g_{\text{FV}}^2(L, L/a)$ and $Z_{\text{FV}}^\phi(L, L/a)$ measured with various $(1/g^2, L/a)$. We also list χ^2/N_{df} in the fit.

We can determine SSFs by using Eqs. (15) and (16). However, they are the SSFs on a lattice. We need to extrapolate the lattice SSFs to the continuum ones. As the preparation, in each set, we line up $g_{\text{FV}}^2(L_0, L_0/a)$ to the specific value. As an example, we consider the set A in Table II. We adopt $u'_0 \equiv 0.6755$ as the specific value. By using SSFs, we can evolve $g_{\text{FV}}^2(L_0, L_0/a) = 0.6752 - 0.6756$ to $g_{\text{FV}}^2(s_0 L_0, s_0 L_0/a) = u'_0$ with some factor s_0 . In this situation, s_0 is nearly equal to 1, so that we can safely use the perturbative expression of the continuum SSFs. By solving $u'_0 = \sigma_{\text{P}}^g(s_0, g_{\text{FV}}^2(L_0, L_0/a))$ numerically with Newton’s method, we determine s_0 . Then, we evaluate the lattice SSFs by

$$\Sigma^g(s, u'_0, a/L_0) = \sigma_{\text{P}}^g(s_0, g_{\text{FV}}^2(sL_0, sL_0/a)) , \quad (29)$$

$$\Sigma^\phi(s, u'_0, a/L_0) = \frac{\sigma_{\text{P}}^\phi(s_0, g_{\text{FV}}^2(sL_0, sL_0/a)) Z_{\text{FV}}^\phi(sL_0, sL_0/a)}{\sigma_{\text{P}}^\phi(s_0, g_{\text{FV}}^2(L_0, L_0/a)) Z_{\text{FV}}^\phi(L_0, L_0/a)} . \quad (30)$$

In the present study, $s \equiv L/L_0$ is a factor greater than 1 but not more than 2. The statistical errors are roughly estimated from

$$\Delta(\Sigma^g(s, u'_0, a/L_0)) = \sqrt{\left[\frac{\partial \sigma_{\text{P}}^g(s, u'_0)}{\partial u} \frac{\partial \sigma_{\text{P}}^g(s_0, u_0)}{\partial u} \Delta(u_0) \right]^2 + \left[\frac{\partial \sigma_{\text{P}}^g(s_0, u_1)}{\partial u} \Delta(u_1) \right]^2} , \quad (31)$$

$$\Delta(\Sigma^\phi(s, u'_0, a/L_0)) = \sqrt{\left[\Delta \left(\frac{\sigma_{\text{P}}^\phi(s_0, u_1)}{\sigma_{\text{P}}^\phi(s_0, u_0)} \right) \frac{v_1}{v_0} \right]^2 + \left[\frac{\sigma_{\text{P}}^\phi(s_0, u_1)}{\sigma_{\text{P}}^\phi(s_0, u_0)} \Delta \left(\frac{v_1}{v_0} \right) \right]^2} . \quad (32)$$

The symbol Δ denotes the statistical error. We refer $g_{\text{FV}}^2(L_0, L_0/a)$ by u_0 , $g_{\text{FV}}^2(sL_0, sL_0/a)$ by u_1 , $Z_{\text{FV}}^\phi(L_0, L_0/a)$ by v_0 , and $Z_{\text{FV}}^\phi(sL_0, sL_0/a)$ by v_1 to simplify the expressions. $\Delta(\sigma_{\text{P}}^\phi(s_0, u_1)/\sigma_{\text{P}}^\phi(s_0, u_0))$ is estimated from

$$\Delta \left(\frac{\sigma_{\text{P}}^\phi(s_0, u_1)}{\sigma_{\text{P}}^\phi(s_0, u_0)} \right) = \sqrt{[E \Delta(u_0)]^2 + \left[\frac{1}{\sigma_{\text{P}}^\phi(s_0, u_0)} \frac{\partial \sigma_{\text{P}}^\phi(s_0, u_1)}{\partial u} \Delta(u_1) \right]^2} , \quad (33)$$

where the coefficient E is defined as

$$E \equiv - \frac{\sigma_{\text{P}}^\phi(s_0, u_1)}{\sigma_{\text{P}}^\phi(s_0, u_0)^2} \frac{\partial \sigma_{\text{P}}^\phi(s_0, u_0)}{\partial u} - \left(\frac{1}{\sigma_{\text{P}}^\phi(s_0, u_0)} \frac{\partial \sigma_{\text{P}}^\phi(s_0, u_1)}{\partial s} - \frac{\sigma_{\text{P}}^\phi(s_0, u_1)}{\sigma_{\text{P}}^\phi(s_0, u_0)^2} \frac{\partial \sigma_{\text{P}}^\phi(s_0, u_0)}{\partial s} \right) \frac{\partial \sigma_{\text{P}}^g(s_0, u_0)/\partial u}{\partial \sigma_{\text{P}}^g(s_0, u_0)/\partial s} . \quad (34)$$

In Tables VII, VIII, IX, X and XI, we give $\Sigma^g(s, u'_0, a/L_0)$ and $\Sigma^\phi(s, u'_0, a/L_0)$ for various $(L_0/a, s)$ of each set. Each set corresponds to $u'_0 = 0.6755$ for set A, $u'_0 = 0.7383$ for set B, $u'_0 = 0.8166$ for set C, $u'_0 = 0.9176$ for set D, and $u'_0 = 1.0595$ for set E.

In Fig. 3, we show the s -dependence of $\Sigma^g(s, u'_0, a/L_0)$ and $\Sigma^\phi(s, u'_0, a/L_0)$ for various $(u'_0, L_0/a)$. While the data points of $\Sigma^\phi(s, u'_0, a/L_0)$ are almost located on a single curve without depending on L_0/a , the data points of $\Sigma^g(s, u'_0, a/L_0)$ show a larger fluctuation. One of the reasons is considered as follows. The renormalized coupling g_{FV}^2 is defined by multiplying L/a to the dimensionless mass gap Ma . As the results, the uncertainty of Ma due to the fit-range dependence is amplified in the value of g_{FV}^2 . However, $\Sigma^g(s, u'_0, a/L_0)$ might have the (L_0/a) -dependence beyond this uncertainty. In Sec. IV B, we discuss the (L_0/a) -dependence of $\Sigma^g(s, u'_0, a/L_0)$ and $\Sigma^\phi(s, u'_0, a/L_0)$, and evaluate the values at $(s, a/L_0) = (2, 0)$.

B. Continuum limit

The continuum limit is nothing less than the limit of $a/L_0 \rightarrow 0$. We extract the values of $\Sigma^{g,\phi}(s, u'_0, a/L_0)$ at $(s, a/L_0) = (2, 0)$ by fit for each u'_0 . We use the fitting forms as

$$\Sigma^g(s, u'_0, a/L_0) = u'_0 + \sum_k W_k(s, a/L_0) \Sigma_k^g(u'_0) , \quad (35)$$

$$\Sigma^\phi(s, u'_0, a/L_0) = 1 + \sum_k W_k(s, a/L_0) \Sigma_k^\phi(u'_0) . \quad (36)$$

The function $W_k(s, a/L_0)$ is defined by

$$W_{(i-1)j_{\text{max}}+j}(s, a/L_0) \equiv (\ln s)^i (a/L_0)^{2j} , \quad (37)$$

for $i = 1, \dots, i_{\text{max}}$ and $j = 0, \dots, j_{\text{max}} - 1$. These are motivated from Eqs. (20), (21) and (22). $\Sigma_k^g(u'_0)$ and $\Sigma_k^\phi(u'_0)$ are free parameters. They are determined for each u'_0 by minimizing χ^2 , in other words, solving the linear simultaneous equation

$$\sum_l A_{kl}^{g,\phi}(u'_0) \Sigma_l^{g,\phi}(u'_0) = B_k^{g,\phi}(u'_0) , \quad (38)$$

with

$$A_{kl}^{g,\phi}(u'_0) \equiv \sum_{s, a/L_0} \frac{W_k(s, a/L_0) W_l(s, a/L_0)}{\Delta (\Sigma^{g,\phi}(s, u'_0, a/L_0))^2} , \quad (39)$$

$$B_k^{g,\phi}(u'_0) \equiv \sum_{s, a/L_0} \frac{(\bar{\Sigma}^{g,\phi}(s, u'_0, a/L_0) - \{u'_0, 1\}) W_k(s, a/L_0)}{\Delta (\Sigma^{g,\phi}(s, u'_0, a/L_0))^2} . \quad (40)$$

Here $\bar{\Sigma}^{g,\phi}(s, u'_0, a/L_0)$ denotes the expectation value of $\Sigma^{g,\phi}(s, u'_0, a/L_0)$. $\{u'_0, 1\}$ means u'_0 for $B_k^g(u'_0)$, and 1 for $B_k^\phi(u'_0)$. The summation is taken over $(s, a/L_0)$ used in the measurement.

We need an attention for the evaluation of the statistical errors of $\Sigma^{g,\phi}(s, u'_0, 0)$. When $(\ln s)$ takes non-zero value, correlation between the fitting parameters must be considered. The variance-covariance matrix for the parameter $\Sigma_k^{g,\phi}(u'_0)$ can be described by $(A^{g,\phi}(u'_0))^{-1}$. Thus, the statistical errors are evaluated by

$$\Delta (\Sigma^{g,\phi}(s, u'_0, 0))^2 = \sum_{k,l} (A^{g,\phi}(u'_0))_{kl}^{-1} W_k(s, 0) W_l(s, 0) . \quad (41)$$

Eqs. (17) and (18) suggest that we can evaluate the β function and the anomalous dimension at $\sigma^g(s, u'_0) = \Sigma^g(s, u'_0, 0)$ with $\Sigma_k^{g,\phi}(u'_0)$ determined by the fit. We evaluate the expectation values by

$$-s \frac{\partial \Sigma^g(s, u'_0, 0)}{\partial s} = -s \sum_k \frac{\partial W_k(s, 0)}{\partial s} \Sigma_k^g(u'_0), \quad (42)$$

$$-s \frac{\partial \ln \Sigma^\phi(s, u'_0, 0)}{\partial s} = -\frac{s}{\Sigma^\phi(s, u'_0, 0)} \sum_k \frac{\partial W_k(s, 0)}{\partial s} \Sigma_k^\phi(u'_0). \quad (43)$$

The statistical error of $-s \partial \Sigma^g(s, u'_0, 0)/\partial s$ is evaluated by

$$\Delta \left(-s \frac{\partial \Sigma^g(s, u'_0, 0)}{\partial s} \right)^2 = s^2 \sum_{k,l} (A^g(u'_0))_{kl}^{-1} \frac{\partial W_k(s, 0)}{\partial s} \frac{\partial W_l(s, 0)}{\partial s}. \quad (44)$$

On the other hands, to evaluate the statistical error of $-s \partial \ln \Sigma^\phi(s, u'_0, 0)/\partial s$, we use an approximation $(\ln \Sigma^\phi) \simeq \Sigma^\phi - 1$, and calculate

$$\begin{aligned} \Delta \left(-s \frac{\partial \ln \Sigma^\phi(s, u'_0, 0)}{\partial s} \right)^2 &\simeq \left(-s \frac{\partial (\Sigma^\phi(s, u'_0, 0) - 1)}{\partial s} \right)^2 \\ &= s^2 \sum_{k,l} (A^\phi(u'_0))_{kl}^{-1} \frac{\partial W_k(s, 0)}{\partial s} \frac{\partial W_l(s, 0)}{\partial s}. \end{aligned} \quad (45)$$

From Tables VII, VIII, IX, X and XI, we find $|\Sigma^\phi - 1| < 0.23$ in $u'_0 = 0.6755 - 1.0595$. To compensate the underestimation due to the approximation, we multiply the factor $1+0.23^2 = 1.0529$ in the evaluation of $\Delta(-s \partial \ln \Sigma^\phi(s, u'_0, 0)/\partial s)$.

In Table XII, we give the fitting results to Eqs. (35) and (36) with $(i_{\max}, j_{\max}) = (2, 2)$. We show $\sigma^g(2, u'_0) = \Sigma^g(2, u'_0, 0)$ and $\sigma^\phi(2, u'_0) = \Sigma^\phi(2, u'_0, 0)$ for each u'_0 . We also list the β function and the anomalous dimension at $\sigma^g(2, u'_0) = \Sigma^g(2, u'_0, 0)$.

C. Scale dependence

We discuss the continuum SSFs with $s = 2$, which are obtained in the analysis of Sec. IV B. In Fig. 4, we give a comparison between the Monte Carlo simulation and the perturbative evaluation. $\sigma^g(2, g_{\text{FV}}^2)$ is shown in the top panel, and $\sigma^\phi(2, g_{\text{FV}}^2)$ in the bottom panel. It can be observed that the perturbative evaluation approaches the result by Monte Carlo simulation with an increase in the order. Moreover, we fit

$$\sigma_{\text{F}}^g(2, u) \equiv u + u^2 \left(\frac{n-2}{2\pi} (\ln 2) \right) + u^3 \left(\frac{n-2}{4\pi^2} (\ln 2) + \frac{(n-2)^2}{4\pi^2} (\ln 2)^2 \right) + \sum_{i=2}^5 u^{i+2} \sigma_i^g, \quad (46)$$

$$\sigma_{\text{F}}^\phi(2, u) \equiv 1 + u \left(-\frac{n-1}{2\pi} (\ln 2) \right) + \sum_{i=1}^4 u^{i+1} \sigma_i^\phi, \quad (47)$$

to the Monte Carlo data, where σ_i^g ($2 \leq i \leq 5$) and σ_i^ϕ ($1 \leq i \leq 4$) are free parameters in the fit. We use the universal forms independent of the renormalization scheme for the first three terms of $\sigma_F^g(2, g_{FV}^2)$, and the first two terms of $\sigma_F^\phi(2, g_{FV}^2)$. χ^2/N_{df} in the fit is 0.40 for $\sigma^g(2, g_{FV}^2)$, and 0.024 for $\sigma^\phi(2, g_{FV}^2)$. The fitting result is also shown in Fig. 4.

We consider the scale dependence of g_{FV}^2 and Z_{FV}^ϕ . The SSFs are determined by the fit to Eqs. (46) and (47), and expected to be sufficiently precise in the range of $g_{FV}^2 = 0.67 - 1.27$. With the SSFs, we determine $g_{FV}^2(2^k L_{\min})$ and $Z_{FV}^\phi(2^k L_{\min})$ ($k = 0, \dots, 5$) by Eqs. (15) and (16). Here L_{\min} is defined by $L_{\min} = 2^{-5} L_{\max}$ with $mL_{\max} = 0.5557(13)$. m is the mass gap in the infinite volume. The value of mL_{\max} corresponds to $g_{FV}^2(L_{\max}) = 1.2680$, and is referred from Ref. [2]. In addition, we set $Z_{FV}^\phi(L_{\max}) = 1.0$. Note that the values of $g_{FV}^2(L_{\max})$ and $Z_{FV}^\phi(L_{\max})$ are set without statistical errors. The statistical errors of $g_{FV}^2(L)$ and $Z_{FV}^\phi(L)$ are recursively estimated by

$$\Delta(g_{FV}^2(L)) = \frac{1}{[\partial\sigma_F^g(2, u)/\partial u]_{u=g_{FV}^2(L)}} \sqrt{\left[\Delta(g_{FV}^2(2L))\right]^2 + \left[\Delta(\sigma_F^g(2, g_{FV}^2(L)))\right]^2}, \quad (48)$$

$$\Delta(Z_{FV}^\phi(L)) = \frac{1}{\sigma_F^\phi(2, g_{FV}^2(L))} \sqrt{\left[\Delta(Z_{FV}^\phi(2L))\right]^2 + \left[\frac{\Delta(\sigma_F^\phi(2, g_{FV}^2(L)))}{\sigma_F^\phi(2, g_{FV}^2(L))} Z_{FV}^\phi(2L)\right]^2}. \quad (49)$$

$\Delta(\sigma_F^{g,\phi}(2, g_{FV}^2(L)))$ denotes the statistical error due to ones of the fitting parameters. For the estimation, we include a contribution from the correlation between the parameters as we have done in Sec. IV B. In Table XIII, the values of $m \times 2^k L_{\min}$, $g_{FV}^2(2^k L_{\min})$ and $Z_{FV}^\phi(2^k L_{\min})$ ($k = 0, \dots, 5$) are listed. In Fig. 5, these data are plotted. We also show the results obtained by numerically integrating Eqs. (13) and (14) from $mL_{\min} = 0.017366$ with the perturbative $\beta_{FV}(g_{FV}^2)$ and $\gamma_{FV}(g_{FV}^2)$. We can confirm a reasonable behavior of the Monte Carlo data in comparison with the perturbative evaluation.

Finally, we discuss the β function and the anomalous dimension. In principle, we can obtain them by differentiating $g_{FV}^2(L)$ and $Z_{FV}^\phi(L)$ with respect to L . However, the function forms of $g_{FV}^2(L)$ and $Z_{FV}^\phi(L)$ are complicated, so that doing the differentiation numerically seems to be difficult. We alternatiely use the data of $\beta_{FV}(\sigma^g(2, u'_0))$ and $\gamma_{FV}(\sigma^g(2, u'_0))$ determined in Sec. IV B. In Fig. 6, the results by the Monte Carlo simulation are shown. The perturbative evaluation is also described for a comparison. We can observe the reasonable behaviors again although the statistical errors are relatively large compared to ones of the SSFs or the renormalized parameters. It is possible to fit $\beta_{FV}(g_{FV}^2)$ and $\gamma_{FV}(g_{FV}^2)$, and determine the coefficients. However, we have only five data points in the present study. It is difficult to determine them with a sufficient statistical precision, so that we do not perform the fit. We leave the precise determination of the coefficients as a future task.

V. CONCLUSION

We have studied the finite box-size effects on the wave-function renormalization of the 2-dimensional $O(3)$ sigma model. We have analyzed the step-scaling functions (SSF), which

was proposed in a successful analysis of the renormalized coupling of the same model [2]. The SSF of the wave-function renormalization factor, Z_{FV}^ϕ , is determined with a sufficient precision and its scale dependence is studied. We have compared the results with the perturbative evaluation and found a good agreement between them. The β function and the anomalous dimension are determined and it is found that their behaviors are also consistent with the perturbative evaluation.

Our analysis supports that the RG description of Z_{FV}^ϕ works well, and thus it gives another evidence for the existence of RG equation, which describes the box-size dependence of the N -point Green function. The concrete construction of the RG equation will be addressed in the forthcoming report [22].

At the end, we give prospective views. The RG equation in few-body quantum systems will be a useful tool for the analysis of spatially extended objects, such as (loosely) bound two or a few-body systems and of the Efimov-like critical behaviors of the system as we have mentioned in Sec. I. The analyses of the finite box-size effects should also have realistic physical meaning, not being an artifact or an systematic error. A well-known example is the finite temperature system, where the finiteness in the imaginary time direction plays a key role. There the RG equation for the box-size parameter must be a new powerful tool for studying the temperature dependences.

Acknowledgments

A part of the numerical calculations was carried out on the super parallel computers, CRAY XC40 at YITP in Kyoto University.

Appendix A: Perturbative evaluation

1. Preparation

To clarify the notation, we give a brief description of the action, Feynman rules, Green functions and boundary condition.

We use the dimensional regularization, so that Eq. (1) must be extended to d -dimensional action,

$$S[\phi] = \frac{1}{2g^2} \int_{\Lambda} d^d z \partial_\mu \phi(z) \cdot \partial_\mu \phi(z) \quad (\mu = 0, \dots, d-1). \quad (\text{A1})$$

Here the system is put on

$$\Lambda = \left\{ z \left| z_0 \in [-T/2, T/2], z_i \in [0, L] \text{ for } i = 1, \dots, d-1 \right. \right\}. \quad (\text{A2})$$

As we have said in Sec. I, a particular attention must be paid for the treatment of zero mode. The zero mode occurs from the degree of freedom where the ϕ field is rotated by a same matrix over all points of the time and space. To separate it, we use an $O(n)$ rotation

matrix Ω which is independent of the space-time points, and parametrize the ϕ field as

$$\phi(z) = \Omega \left(\sqrt{1 - g^2 \boldsymbol{\pi}^2(z)}, g \boldsymbol{\pi}(z) \right)^T. \quad (\text{A3})$$

$\boldsymbol{\pi}(z) = (\pi_i(z), i = 1, \dots, n-1)$ is the $(n-1)$ -component field. In the following, we use the bullet point symbol also for the scalar product of $(n-1)$ -component vectors. As long as there is no confusion, we use the abbreviation such as $\boldsymbol{\pi}^2 = \boldsymbol{\pi} \cdot \boldsymbol{\pi}$. According to Ref. [14, 23], we consider the identity,

$$1 = \int d^n \mathbf{m} \delta^n \left(\mathbf{m} - \frac{1}{TL^{d-1}} \int d^d z \phi(z) \right). \quad (\text{A4})$$

Substituting Eq. (A3) to Eq. (A4), we obtain

$$1 = S_{n-1} \left[\prod_{i=1}^{n-1} \delta \left(-\frac{g}{TL^{d-1}} \int d^d z \pi_i \right) \right] \exp \left[-\frac{(n-1)g^2}{2TL^{d-1}} \int d^d z \boldsymbol{\pi}^2 \right], \quad (\text{A5})$$

where S_{n-1} is the surface area of $(n-1)$ -dimensional unit sphere. Note that the identity (A5) is satisfied even in the interior of path integration with respect to the $\boldsymbol{\pi}$ field. By applying Eq. (A5) to the partition function, we have

$$\begin{aligned} \mathcal{Z} &= \int \left[\delta(\phi^2(z) - 1) d\phi(z) \right] e^{-S[\phi]} \\ &= \int \left[\frac{g d\boldsymbol{\pi}(z)}{\sqrt{1 - g^2 \boldsymbol{\pi}^2(z)}} \right] \exp \left[-\int d^d z \left\{ \frac{1}{2} \partial_\mu \boldsymbol{\pi} \cdot \partial_\mu \boldsymbol{\pi} + \frac{g^2}{8} \frac{(\partial_\mu \boldsymbol{\pi}^2)^2}{1 - g^2 \boldsymbol{\pi}^2} \right\} \right] \\ &= \int [g d\boldsymbol{\pi}(z)] \exp \left[-\int d^d z \left\{ \frac{1}{2} \partial_\mu \boldsymbol{\pi} \cdot \partial_\mu \boldsymbol{\pi} + \frac{g^2}{8} \frac{(\partial_\mu \boldsymbol{\pi}^2)^2}{1 - g^2 \boldsymbol{\pi}^2} + \frac{1}{2} \delta^d(0) \ln(1 - g^2 \boldsymbol{\pi}^2) \right\} \right] \\ &= S_{n-1} \int [g d\boldsymbol{\pi}(z)] \left[\prod_{i=1}^{n-1} \delta \left(-\frac{g}{TL^{d-1}} \int d^d z \pi_i \right) \right] \\ &\quad \times \exp \left[-\int d^d z \left\{ \frac{1}{2} \partial_\mu \boldsymbol{\pi} \cdot \partial_\mu \boldsymbol{\pi} + \frac{g^2}{8} \frac{(\partial_\mu \boldsymbol{\pi}^2)^2}{1 - g^2 \boldsymbol{\pi}^2} + \frac{1}{2} \delta^d(0) \ln(1 - g^2 \boldsymbol{\pi}^2) + \frac{(n-1)g^2}{2TL^{d-1}} \boldsymbol{\pi}^2 \right\} \right]. \end{aligned} \quad (\text{A6})$$

The factor of delta functions excludes the zero mode of $\boldsymbol{\pi}$ field. As the compensation, we must include an extra interaction term, $\frac{(n-1)g^2}{2TL^{d-1}} \boldsymbol{\pi}^2$.

Due to Eq. (A3), $\boldsymbol{\pi}$ must satisfy the condition, $|\boldsymbol{\pi}| \leq 1/g$. However, starting from the final expression of Eq. (A6), we are no longer constrained by the condition. It can be also understood from the free-field part of Eq. (A6) that $|\boldsymbol{\pi}| \leq 1$ gives a main contribution to the path integration, and $|\boldsymbol{\pi}| \sim 1/g$ does an exponentially small contribution. Thus, the range of integration can be safely extended to $|\boldsymbol{\pi}| < \infty$. See Ref. [24] for more details.

We have $\delta^d(0) = 0$ with the dimensional regularization¹. Thus, we need not consider the interaction due to the integral measure, $\frac{1}{2} \delta^d(0) \ln(1 - g^2 \boldsymbol{\pi}^2)$, in the following discussion.

¹ We can write as $\delta^d(0) = \int_{-\infty}^{\infty} \frac{d^d k}{(2\pi)^d} 1 = \int_{-\infty}^{\infty} \frac{d^d k}{(2\pi)^d} \frac{k^2 + \alpha^2}{k^2 + \alpha^2} = \int_{-\infty}^{\infty} \frac{d^d k}{(2\pi)^d} (k^2 + \alpha^2) \int_0^{\infty} dt e^{-(k^2 + \alpha^2)t}$

Note that if we use the lattice regularization, the IR cutoff mass g/a is introduced due to $\delta^2(0) = 1/a^2$ and enables to isolate the momentum zero mode in a finite volume. The action for the $\boldsymbol{\pi}$ field can be written as

$$\begin{aligned} S[\boldsymbol{\pi}] &= \int d^d z \left[\frac{1}{2} \partial_\mu \boldsymbol{\pi} \cdot \partial^\mu \boldsymbol{\pi} + \frac{(n-1)g^2}{2TL^{d-1}} \boldsymbol{\pi}^2 + \frac{g^2}{8} \frac{(\partial_\mu \boldsymbol{\pi}^2)^2}{1-g^2 \boldsymbol{\pi}^2} \right] \\ &= \int d^d z \left[\frac{1}{2} \partial_\mu \boldsymbol{\pi} \cdot \partial^\mu \boldsymbol{\pi} + \frac{(n-1)g^2}{2TL^{d-1}} \boldsymbol{\pi}^2 + \frac{g^2}{8} (\partial_\mu \boldsymbol{\pi}^2)^2 + \mathcal{O}(g^4) \right]. \end{aligned} \quad (\text{A7})$$

In Fig. 7, we summarize the Feynman rules which we can interpret from this action. The details of the $\boldsymbol{\pi}$ propagator, $G(x, y)$, are discussed a bit later.

We define the expectation value of an operator O as

$$\begin{aligned} \langle O \rangle &= \frac{S_{n-1}}{\mathcal{Z}} \int [g d\boldsymbol{\pi}(z)] \left[\prod_{i=1}^{n-1} \delta \left(-\frac{g}{TL^{d-1}} \int d^d z \pi_i \right) \right] e^{-S_\pi} \times O \\ &= \frac{S_{n-1}}{\mathcal{Z}} \int [g d\boldsymbol{\pi}(z)] \left[\prod_{i=1}^{n-1} \delta \left(-\frac{g}{TL^{d-1}} \int d^d z \pi_i \right) \right] e^{-\int d^d z \frac{1}{2} \partial_\mu \boldsymbol{\pi} \cdot \partial_\mu \boldsymbol{\pi}} \\ &\quad \times O \left\{ 1 - g^2 \int d^d z \left[\frac{(n-1)}{2TL^{d-1}} \boldsymbol{\pi}^2 + \frac{1}{8} (\partial_\mu \boldsymbol{\pi}^2)^2 \right] + \mathcal{O}(g^4) \right\}. \end{aligned} \quad (\text{A8})$$

In the following, the coefficient of $(g^2)^i$ is referred by $\langle O \rangle_i$ with a non-negative integer i .

From Eq. (A8), the free $\boldsymbol{\pi}$ propagator,

$$\langle \pi_i(x) \pi_j(y) \rangle_0 = \delta_{ij} G(x; y), \quad (\text{A9})$$

satisfies²

$$\square_x G(x; y) = -\delta^d(x - y) + \frac{1}{TL^{d-1}}. \quad (\text{A10})$$

To determine $G(x; y)$, the boundary condition must be set. We adopt the NBC for the temporal direction, and the PBC for the spatial direction,

$$\begin{aligned} \frac{\partial}{\partial x_0} G(x_0, \mathbf{x}; y_0, \mathbf{y}) &= 0 \quad (x_0 = \pm T/2), \quad \frac{\partial}{\partial y_0} G(x_0, \mathbf{x}; y_0, \mathbf{y}) = 0 \quad (y_0 = \pm T/2), \\ G(x_0, \mathbf{x} + L\mathbf{n}_x; y_0, \mathbf{y} + L\mathbf{n}_y) &= G(x_0, \mathbf{x}; y_0, \mathbf{y}) \quad (\mathbf{n}_x, \mathbf{n}_y \in \mathbb{Z}^{d-1}). \end{aligned} \quad (\text{A11})$$

with an arbitrary non-zero parameter α . After changing the order of integration and doing the k -integration, we have $\delta^d(0) = \frac{1}{2^d \pi^{d/2}} \left[\frac{d}{2} \int_0^\infty dt e^{-\alpha^2 t} t^{-d/2-1} + \alpha^2 \int_0^\infty dt e^{-\alpha^2 t} t^{(-d/2+1)-1} \right]$. When $\text{Re}(d) < 0$, these integrations converge, and we obtain $\delta^d(0) = 0$. Considering $\delta^d(0)$ as an analytical function of d , we can continue it to $\text{Re}(d) \geq 0$, analytically. Then, we have $\delta^d(0) = 0$ for any complex dimension d .

² The constant term, $\frac{1}{TL^{d-1}}$, appears due to the exclusion of zero mode. Consider a formal solution $\bar{G}(z) = \frac{1}{TL^{d-1}} \sum_{p \neq 0} \frac{e^{ip \cdot z}}{p^2}$. One can confirm the appearance of the constant term from the calculation of $\square_z \bar{G}(z) = \frac{1}{TL^{d-1}} \sum_{p \neq 0} \frac{\square_z e^{ip \cdot z}}{p^2} = -\frac{1}{TL^{d-1}} \sum_p e^{ip \cdot z} + \frac{1}{TL^{d-1}} \sum_{p=0} e^{ip \cdot z} = -\delta^d(z) + \frac{1}{TL^{d-1}}$.

Then, $G(x; y)$ can be written as

$$G(x; y) = \sum_{(m, \mathbf{n}) \neq (0, \mathbf{0})} \frac{1}{\lambda_{m\mathbf{n}}^2} \phi_{m\mathbf{n}}^*(y) \phi_{m\mathbf{n}}(x) , \quad (\text{A12})$$

with

$$\lambda_{m\mathbf{n}}^2 = p_m^2 + \mathbf{q}_{\mathbf{n}}^2 \quad \left(p_m = \frac{\pi m}{T}, \quad \mathbf{q}_{\mathbf{n}} = \frac{2\pi \mathbf{n}}{L} \mid m \in \mathbb{Z}, \quad \mathbf{n} \in \mathbb{Z}^{d-1} \right) \quad (\text{A13})$$

and

$$\phi_{m\mathbf{n}}(x) = \begin{cases} \sqrt{1/(TL^{d-1})} e^{i\mathbf{q}_{\mathbf{n}} \cdot \mathbf{x}} & (m = 0) \\ \sqrt{2/(TL^{d-1})} e^{i\mathbf{q}_{\mathbf{n}} \cdot \mathbf{x}} \cos(p_m x_0) & (m : \text{even but not zero}) \\ \sqrt{2/(TL^{d-1})} e^{i\mathbf{q}_{\mathbf{n}} \cdot \mathbf{x}} \sin(p_m x_0) & (m : \text{odd}) \end{cases} . \quad (\text{A14})$$

$\lambda_{m\mathbf{n}}^2$ and $\phi_{m\mathbf{n}}(x)$ are the eigenvalue and eigenfunction of

$$\square_x \phi(x) = -\lambda^2 \phi(x) \quad (\text{A15})$$

with the boundary condition

$$\frac{\partial}{\partial x_0} \phi(x_0, \mathbf{x}) = 0 \quad (x_0 = \pm T/2), \quad \phi(x_0, \mathbf{x} + L\mathbf{n}_x) = \phi(x_0, \mathbf{x}) \quad (\mathbf{n}_x \in \mathbb{Z}^{d-1}) . \quad (\text{A16})$$

The normalization of $\phi_{m\mathbf{n}}(x)$ is taken such that the orthonormal condition

$$\int_{\Lambda} d^d x \phi_{m\mathbf{n}}^*(x) \phi_{m'\mathbf{n}'}(x) = \delta_{mm'} \delta_{\mathbf{n}\mathbf{n}'} \quad (\text{A17})$$

is satisfied.

It is useful to separate $G(x; y)$ as

$$G(x; y) = G_Z(x_0; y_0) + G_N(x; y) , \quad (\text{A18})$$

where $G_Z(x_0; y_0)$ is a contribution from the momentum zero mode ($m \neq 0, \mathbf{n} = \mathbf{0}$)

$$G_Z(x_0; y_0) \equiv \sum_{m \neq 0} \frac{1}{\lambda_{m\mathbf{0}}^2} \phi_{m\mathbf{0}}^*(y) \phi_{m\mathbf{0}}(x) , \quad (\text{A19})$$

and $G_N(x; y)$ is one from the momentum non-zero mode ($\mathbf{n} \neq \mathbf{0}$)

$$G_N(x; y) \equiv \sum_m \sum_{\mathbf{n} \neq \mathbf{0}} \frac{1}{\lambda_{m\mathbf{n}}^2} \phi_{m\mathbf{n}}^*(y) \phi_{m\mathbf{n}}(x) . \quad (\text{A20})$$

After some calculations, we obtain

$$G_Z(x_0; y_0) = \frac{1}{L^{d-1}} \left(-\frac{|x_0 - y_0|}{2} + \frac{x_0^2 + y_0^2}{2T} + \frac{T}{12} \right) , \quad (\text{A21})$$

$$G_N(x; y) = \sum_{m=-\infty}^{\infty} \{ R(x_0 - y_0 + 2mT, \mathbf{x} - \mathbf{y}) + R(x_0 + y_0 + (2m + 1)T, \mathbf{x} - \mathbf{y}) \} , \quad (\text{A22})$$

with the non-zero mode propagator in the infinite temporal extent,

$$R(z) \equiv \frac{1}{2L^{d-1}} \sum_{\mathbf{q}_n \neq \mathbf{0}} \frac{1}{|\mathbf{q}_n|} e^{-|\mathbf{q}_n||z_0| + i\mathbf{q}_n \cdot \mathbf{z}} . \quad (\text{A23})$$

Eq. (A22) can be interpreted that $R(z)$ is padded in the temporal extent T in such a way as to satisfy the NBC. In addition, if we use the zero mode propagator in the infinite temporal extent,

$$r(z_0) = \frac{1}{2L^{d-1}} \lim_{\omega \rightarrow 0^+} \frac{1}{\omega} e^{-\omega|z_0|} , \quad (\text{A24})$$

instead of $R(z)$ in Eq. (A22), we can reproduce Eq. (A21).

The $O(n)$ -invariant 2-point Green function defined by Eq. (4) can be written as

$$\begin{aligned} G_{\text{inv}}(x; y) &= 1 + g^2 \left(\langle \boldsymbol{\pi}(x) \cdot \boldsymbol{\pi}(y) \rangle - \frac{1}{2} \langle \boldsymbol{\pi}^2(x) \rangle - \frac{1}{2} \langle \boldsymbol{\pi}^2(y) \rangle \right) \\ &\quad + g^4 \left(\frac{1}{4} \langle \boldsymbol{\pi}^2(x) \boldsymbol{\pi}^2(y) \rangle - \frac{1}{8} \langle \boldsymbol{\pi}^4(x) \rangle - \frac{1}{8} \langle \boldsymbol{\pi}^4(y) \rangle \right) + \mathcal{O}(g^6) \\ &= 1 + g^2 \left(\langle \boldsymbol{\pi}(x) \cdot \boldsymbol{\pi}(y) \rangle_0 - \frac{1}{2} \langle \boldsymbol{\pi}^2(x) \rangle_0 - \frac{1}{2} \langle \boldsymbol{\pi}^2(y) \rangle_0 \right) \\ &\quad + g^4 \left(\langle \boldsymbol{\pi}(x) \cdot \boldsymbol{\pi}(y) \rangle_1 - \frac{1}{2} \langle \boldsymbol{\pi}^2(x) \rangle_1 - \frac{1}{2} \langle \boldsymbol{\pi}^2(y) \rangle_1 \right. \\ &\quad \left. + \frac{1}{4} \langle \boldsymbol{\pi}^2(x) \boldsymbol{\pi}^2(y) \rangle_0 - \frac{1}{8} \langle \boldsymbol{\pi}^4(x) \rangle_0 - \frac{1}{8} \langle \boldsymbol{\pi}^4(y) \rangle_0 \right) + \mathcal{O}(g^6) . \quad (\text{A25}) \end{aligned}$$

The final expression of Eq. (A25) is evaluated in Sec. A 2 and A 3, perturbatively.

2. Evaluation at $\mathcal{O}(g^2)$

It is instructive to follow the derivation of the $\mathcal{O}(g^2)$ contribution to $O(n)$ -invariant 2-point Green function. The contribution is given by the second term in Eq. (A25). Corresponding to $\langle \boldsymbol{\pi}(x) \cdot \boldsymbol{\pi}(y) \rangle_0$, $\langle \boldsymbol{\pi}^2(x) \rangle_0$ and $\langle \boldsymbol{\pi}^2(y) \rangle_0$, we refer these contributions by ‘‘a’’, ‘‘b’’ and ‘‘c’’, respectively. The diagrammatic description is given in Fig. 8. We project the total momentum in the external line to zero. Each contribution can be calculated from

$$\begin{aligned} P_{\text{a}}(\tau) &= \frac{1}{L^{2(d-1)}} \int d^{d-1} \mathbf{x} \int d^{d-1} \mathbf{y} G(x; y) |_{x_0=-\tau, y_0=+\tau} , \\ P_{\text{b}}(\tau) &= \frac{1}{L^{2(d-1)}} \int d^{d-1} \mathbf{x} \int d^{d-1} \mathbf{y} G(x; x) |_{x_0=-\tau} , \\ P_{\text{c}}(\tau) &= \frac{1}{L^{2(d-1)}} \int d^{d-1} \mathbf{x} \int d^{d-1} \mathbf{y} G(y; y) |_{y_0=+\tau} , \quad (\text{A26}) \end{aligned}$$

except for the coefficient in Eq. (A25), the coefficient in the brace of Eq. (A8), the multiplicity of the spin component and the statistical factor. Here we adopt $x_0 = -\tau$ and $y_0 = +\tau$.

We need not consider to the momentum non-zero mode for $P_a(\tau)$,

$$P_a(\tau) = G_Z(x_0; y_0) |_{x_0=-\tau, y_0=+\tau} = \frac{1}{L^{d-1}} \left(-|\tau| + \frac{\tau^2}{T} + \frac{T}{12} \right). \quad (\text{A27})$$

On the other hands, the momentum non-zero mode is needed for $P_b(\tau)$ and $P_c(\tau)$. Dropping the terms which are exponentially small in $T \rightarrow \infty$, we have

$$P_b(\tau) = G_Z(x_0; x_0) |_{x_0=-\tau} + G_N(x; x) |_{x_0=-\tau} = \frac{1}{L^{d-1}} \left(\frac{\tau^2}{T} + \frac{T}{12} \right) + R(0), \quad (\text{A28})$$

$$P_c(\tau) = G_Z(y_0; y_0) |_{y_0=+\tau} + G_N(y; y) |_{y_0=+\tau} = \frac{1}{L^{d-1}} \left(\frac{\tau^2}{T} + \frac{T}{12} \right) + R(0). \quad (\text{A29})$$

In the derivation of Eqs. (A28) and (A29), the condition $-T/2 < \tau < T/2$ is used.

The factors multiplying to each $P(\tau)$ are given by

$$\begin{aligned} F_a &= g^2 \times 1 \times (n-1) \times 1, \\ F_b &= (-g^2/2) \times 1 \times (n-1) \times 1, \\ F_c &= (-g^2/2) \times 1 \times (n-1) \times 1. \end{aligned} \quad (\text{A30})$$

Thus, the total contribution at $\mathcal{O}(g^2)$ can be written as

$$\begin{aligned} &g^2 \frac{1}{L^{2(d-1)}} \int d^{d-1} \mathbf{x} \int d^{d-1} \mathbf{y} \langle \phi(x) \cdot \phi(y) \rangle_1 \\ &= F_a P_a(\tau) + F_b P_b(\tau) + F_c P_c(\tau) \\ &= g^2 \left[-(n-1) R(0) - (n-1) \left(\frac{|\tau|}{L^{d-1}} \right) \right]. \end{aligned} \quad (\text{A31})$$

Note that the terms proportional to T cancel. This fact means that the divergence at $T \rightarrow \infty$ (IR divergence) vanishes by treating the $O(n)$ -invariant Green function. It should be also noted that the terms proportional to τ^2 cancel. The appearance of the τ^2 terms in $P_b(\tau)$ and $P_c(\tau)$ is due to the use of NBC. Such a cancellation does not occur if we use the periodic boundary condition for the temporal direction.

3. Evaluation at $\mathcal{O}(g^4)$

The $\mathcal{O}(g^4)$ contribution to $O(n)$ -invariant 2-point Green function is given by the third term in Eq. (A25). Corresponding to $\langle \boldsymbol{\pi}(x) \cdot \boldsymbol{\pi}(y) \rangle_1$, $\langle \boldsymbol{\pi}^2(x) \rangle_1$, $\langle \boldsymbol{\pi}^2(y) \rangle_1$, $\langle \boldsymbol{\pi}^2(x) \boldsymbol{\pi}^2(y) \rangle_0$, $\langle \boldsymbol{\pi}^4(x) \rangle_0$ and $\langle \boldsymbol{\pi}^4(y) \rangle_0$, we refer these contributions by ‘‘a’’, ‘‘b’’, ‘‘c’’, ‘‘d’’, ‘‘e’’ and ‘‘f’’, respectively. Moreover, we subdivide each contribution into some groups based on the type of interaction, or the pattern for contraction. The diagrammatic description is given in Fig. 9. We project the total momentum in the external line to zero, again, and introduce the abridged notation,

$$\begin{aligned} \text{Int}_2[f(x, y)] &\equiv \frac{1}{L^{2(d-1)}} \int d^{d-1} \mathbf{x} \int d^{d-1} \mathbf{y} [f(x, y)]_{x_0=-\tau, y_0=+\tau}, \\ \text{Int}_3[f(x, y, z)] &\equiv \frac{1}{L^{2(d-1)}} \int d^{d-1} \mathbf{x} \int d^{d-1} \mathbf{y} \int d^d z [f(x, y, z)]_{x_0=-\tau, y_0=+\tau}. \end{aligned} \quad (\text{A32})$$

Then, each contribution can be calculated from

$$\begin{aligned}
P_{a0}(\tau) &= \text{Int}_3[\partial_\mu^2 G(x; z) G(z; y) \partial_\mu^1 G(z; z) + \partial_\mu^2 G(x; z) G(z; y) \partial_\mu^2 G(z; z) \\
&\quad + G(x; z) \partial_\mu^1 G(z; y) \partial_\mu^1 G(z; z) + G(x; z) \partial_\mu^1 G(z; y) \partial_\mu^2 G(z; z)] \\
P_{a1}(\tau) &= \text{Int}_3[\partial_\mu^2 G(x; z) G(z; y) \partial_\mu^2 G(z; z) + \partial_\mu^2 G(x; z) \partial_\mu^1 G(z; y) G(z; z) \\
&\quad + G(x; z) G(z; y) \partial_\mu^1 \partial_\mu^2 G(z; z) + G(x; z) \partial_\mu^1 G(z; y) \partial_\mu^1 G(z; z)] \\
P_{a2}(\tau) &= \text{Int}_3[G(x; z) G(z; y)] \\
P_{b0}(\tau) &= \text{Int}_3[\partial_\mu^2 G(x; z) G(z; x) \partial_\mu^1 G(z; z) + \partial_\mu^2 G(x; z) G(z; x) \partial_\mu^2 G(z; z) \\
&\quad + G(x; z) \partial_\mu^1 G(z; x) \partial_\mu^1 G(z; z) + G(x; z) \partial_\mu^1 G(z; x) \partial_\mu^2 G(z; z)] \\
P_{b1}(\tau) &= \text{Int}_3[\partial_\mu^2 G(x; z) G(z; x) \partial_\mu^2 G(z; z) + \partial_\mu^2 G(x; z) \partial_\mu^1 G(z; x) G(z; z) \\
&\quad + G(x; z) G(z; x) \partial_\mu^1 \partial_\mu^2 G(z; z) + G(x; z) \partial_\mu^1 G(z; x) \partial_\mu^1 G(z; z)] \\
P_{b2}(\tau) &= \text{Int}_3[G(x; z) G(z; x)] \\
P_{c0}(\tau) &= \text{Int}_3[\partial_\mu^2 G(y; z) G(z; y) \partial_\mu^1 G(z; z) + \partial_\mu^2 G(y; z) G(z; y) \partial_\mu^2 G(z; z) \\
&\quad + G(y; z) \partial_\mu^1 G(z; y) \partial_\mu^1 G(z; z) + G(y; z) \partial_\mu^1 G(z; y) \partial_\mu^2 G(z; z)] \\
P_{c1}(\tau) &= \text{Int}_3[\partial_\mu^2 G(y; z) G(z; y) \partial_\mu^2 G(z; z) + \partial_\mu^2 G(y; z) \partial_\mu^1 G(z; y) G(z; z) \\
&\quad + G(y; z) G(z; y) \partial_\mu^1 \partial_\mu^2 G(z; z) + G(y; z) \partial_\mu^1 G(z; y) \partial_\mu^1 G(z; z)] \\
P_{c2}(\tau) &= \text{Int}_3[G(y; z) G(z; y)] \\
P_{d0}(\tau) &= \text{Int}_2[G(x; x) G(y; y)] \\
P_{d1}(\tau) &= \text{Int}_2[G(x; y) G(x; y)] \\
P_{e0}(\tau) &= \text{Int}_2[G(x; x) G(x; x)] \\
P_{e1}(\tau) &= \text{Int}_2[G(x; x) G(x; x)] \\
P_{f0}(\tau) &= \text{Int}_2[G(y; y) G(y; y)] \\
P_{f1}(\tau) &= \text{Int}_2[G(y; y) G(y; y)] \tag{A33}
\end{aligned}$$

except for the coefficient in Eq. (A25), the coefficient in the brace of Eq. (A8), the multiplicity of the spin component and the statistical factor. Here the superscript in partial differential symbol means

$$\partial_\mu^1 G(u, v) \equiv \frac{\partial G(u, v)}{\partial u^\mu}, \quad \partial_\mu^2 G(u, v) \equiv \frac{\partial G(u, v)}{\partial v^\mu}. \tag{A34}$$

The explicit forms of each $P(\tau)$ in Eq. (A33) and the factor to be multiplied F are summarized in Table XIV. Note that $R(x_0 + y_0 \pm T, \mathbf{x} - \mathbf{y})$ in Eq. (A20) cannot be ignored for the derivation of some of $P(\tau)$ at this order. In addition, it should be also noted that $\partial_0^1 \partial_0^2 G_Z(x_0; y_0) |_{x_0=y_0} = \frac{1}{L^{d-1}} \delta(0)$ vanishes due to $\delta(0) = 0$ with the dimensional regularization.

The total contribution at $\mathcal{O}(g^4)$ can be written as

$$g^4 \frac{1}{L^{2(d-1)}} \int d^{d-1} \mathbf{x} \int d^{d-1} \mathbf{y} \langle \phi(\mathbf{x}) \cdot \phi(\mathbf{y}) \rangle_1$$

$$= g^4 \left[\frac{(n-1)}{2} R(0)^2 + (n-1) R(0) \left(\frac{|\tau|}{L^{d-1}} \right) + \frac{(n-1)^2}{2} \left(\frac{|\tau|}{L^{d-1}} \right)^2 \right]. \quad (\text{A35})$$

4. Evaluation of $R(0)$

We evaluate $R(0)$ which appears in Eqs. (A31) and (A35). Discussion in this subsection is based on Ref. [20]. From Eq. (A23), we have

$$\begin{aligned} R(z) &= \frac{1}{L^{d-1}} \sum_{\mathbf{q}_n \neq \mathbf{0}} \int_{-\infty}^{\infty} \frac{dq_0}{2\pi} \frac{1}{q_0^2 + \mathbf{q}_n^2} e^{iq_0 z_0 + i\mathbf{q}_n \cdot \mathbf{z}} \\ &= \int_0^{\infty} d\lambda \left[\int_{-\infty}^{\infty} \frac{dq_0}{2\pi} e^{-\lambda q_0^2 + iq_0 z_0} \right] \times \left[\frac{1}{L^{d-1}} \sum_{\mathbf{q}_n \neq \mathbf{0}} e^{-\lambda \mathbf{q}_n^2 + i\mathbf{q}_n \cdot \mathbf{z}} \right] \\ &= \int_0^{\infty} d\lambda \left[(4\pi\lambda)^{-\frac{1}{2}} e^{-\frac{z_0^2}{4\lambda}} \right] \times \left[(4\pi\lambda)^{-\frac{d-1}{2}} \sum_{\mathbf{w} \in \mathbb{Z}^{d-1}} e^{-\frac{(\mathbf{z} + L\mathbf{w})^2}{4\lambda}} - \frac{1}{L^{d-1}} \right]. \quad (\text{A36}) \end{aligned}$$

We change the variable from λ to $u \equiv 4\pi\lambda/L^2$. Then, we have

$$R(z) \mu^{-(d-2)} = \frac{1}{4\pi(\mu L)^{d-2}} \int_0^{\infty} du u^{-\frac{1}{2}} e^{-\frac{\pi z_0^2}{L^2 u}} \left[u^{-\frac{d-1}{2}} \prod_{\mu=1}^{d-1} \left\{ \sum_{w_\mu=-\infty}^{\infty} e^{-\pi \frac{(z_\mu/L + w_\mu)^2}{u}} \right\} - 1 \right], \quad (\text{A37})$$

where arbitrary scale μ with a mass dimension is introduced to make $R(z)$ dimensionless. μ is called renormalization scale.

We consider the case of $z = 0$. We define the function

$$S(u) \equiv \sum_{n=-\infty}^{\infty} e^{-\pi u n^2}. \quad (\text{A38})$$

Using the relation $S(u) = u^{-1/2} S(u^{-1})$, we obtain

$$R(0) \mu^{-(d-2)} = \frac{1}{4\pi(\mu L)^{d-2}} \int_0^{\infty} du u^{-1/2} \left[S(u)^{d-1} - 1 \right]. \quad (\text{A39})$$

Moreover, we introduce the notation

$$[f(u)]_{\text{sub}} = \begin{cases} f(u) - [f(u)]_0 & (0 < u < 1) \\ f(u) - [f(u)]_{\infty} & (1 < u) \end{cases}, \quad (\text{A40})$$

where $[f(u)]_0$ and $[f(u)]_{\infty}$ denote the leading asymptotic parts of $f(u)$ at $u \rightarrow 0$ and $u \rightarrow \infty$, respectively. Then, Eq. (A39) can be rewritten as

$$R(0) \mu^{-(d-2)} = \frac{1}{2\pi(\mu L)^{d-2}} \left[-\frac{1}{d-2} - 1 + \frac{1}{2} \int_0^{\infty} du u^{-1/2} [S(u)^{d-1}]_{\text{sub}} \right]. \quad (\text{A41})$$

We expand $S(u)^{d-1}$ with respect to $(d-2)$, and obtain

$$R(0) \mu^{-(d-2)} = \frac{1}{2\pi(\mu L)^{d-2}} \left\{ -\frac{1}{d-2} - 1 + \sum_{j=0}^{\infty} (d-2)^j \frac{X_j}{j!} \right\}, \quad (\text{A42})$$

with

$$X_j \equiv \frac{1}{2} \int_0^{\infty} du u^{-1/2} \left[S(u) (\ln S(u))^j \right]_{\text{sub}}. \quad (\text{A43})$$

As we will see later, X_0 and X_1 do not appear in the final expression of the β function and anomalous dimension up to the $\mathcal{O}(g^6)$ order of the renormalization factor. Thus, we do not give the numerical values of X_0 and X_1 . We add that X_0 can be written in an analytical form

$$X_0 = 1 - \frac{1}{2} \left(\ln 4\pi + \Gamma'(1) \right). \quad (\text{A44})$$

Finally, expanding $(\mu L)^{-(d-2)}$ with respect to $(d-2)$, we obtain

$$R(0) \mu^{-(d-2)} = \frac{1}{2\pi} \left\{ -\frac{1}{d-2} + Y_0(\mu L) + (d-2) Y_1(\mu L) + \mathcal{O}((d-2)^2) \right\}, \quad (\text{A45})$$

where we use the following functions,

$$Y_0(\mu L) \equiv (X_0 - 1) + (\ln \mu L), \quad (\text{A46})$$

$$Y_1(\mu L) \equiv X_1 - (X_0 - 1)(\ln \mu L) - \frac{1}{2}(\ln \mu L)^2. \quad (\text{A47})$$

5. Renormalization in MS scheme

In Eq. (A25) with Eqs. (A31) and (A35), the $O(n)$ -invariant 2-point Green function was given as a series of the bare coupling g^2 . It might be preferable to rewrite in terms of the renormalized coupling. As the UV property is not affected by properties of the box such as the size or the boundary condition, it is possible to use the MS scheme for the renormalization. The $\mathcal{O}(g^6)$ renormalization factor on the $O(n)$ sigma model has been already given in Ref. [25]. The renormalization is done by the replacement

$$g^2 \mu^{d-2} = Z_{\text{MS}}^g g_{\text{MS}}^2, \quad (\text{A48})$$

$$\phi(z) = (Z_{\text{MS}}^\phi)^{1/2} \phi_{\text{MS}}(z), \quad (\text{A49})$$

with

$$\begin{aligned} Z_{\text{MS}}^g &= 1 + \frac{n-2}{2\pi(d-2)} g_{\text{MS}}^2 + \left[\frac{n-2}{8\pi^2(d-2)} + \frac{(n-2)^2}{4\pi^2(d-2)^2} \right] g_{\text{MS}}^4 \\ &\quad + \left[\frac{(n-2)(n+2)}{96\pi^3(d-2)} + \frac{7(n-2)^2}{48\pi^3(d-2)^2} + \frac{(n-2)^3}{8\pi^3(d-2)^3} \right] g_{\text{MS}}^6 + \mathcal{O}(g_{\text{MS}}^8), \end{aligned} \quad (\text{A50})$$

$$\begin{aligned} Z_{\text{MS}}^\phi &= 1 + \frac{n-1}{2\pi(d-2)} g_{\text{MS}}^2 + \frac{(n-1)(n-\frac{3}{2})}{4\pi^2(d-2)^2} g_{\text{MS}}^4 \\ &\quad + \left[\frac{(n-1)(n-2)}{32\pi^3(d-2)} + \frac{(n-1)(n-2)}{24\pi^3(d-2)^2} + \frac{(n-1)(n^2 - \frac{19}{6}n + \frac{5}{2})}{8\pi^3(d-2)^3} \right] g_{\text{MS}}^6 + \mathcal{O}(g_{\text{MS}}^8). \end{aligned} \quad (\text{A51})$$

μ , which was introduced in Sec. A 4, is also used to make g_{MS}^2 dimensionless. Note that the MS scheme focuses on only the elimination of UV divergence and thus the coefficients in Eqs. (A50) and (A51) contain only the pole terms.

Using Eqs. (A48) and (A50), the zero-momentum projected $O(n)$ -invariant Green function $G_{\text{inv}}(x_0; y_0) |_{x_0=-\tau, y_0=+\tau}$ can be rewritten as

$$\begin{aligned}
& 1 + g_{\text{MS}}^2 \left[\left(\frac{n-1}{2\pi(d-2)} - \frac{n-1}{2\pi} Y_0(\mu L) - \frac{(d-2)(n-1)}{2\pi} Y_1(\mu L) \right) \right. \\
& \quad \left. + \left(-(n-1) + (d-2)(n-1)(\ln \mu L) \right) \left(\frac{|\tau|}{L} \right) \right] \\
& + g_{\text{MS}}^4 \left[\left(\frac{(n-1)(n-\frac{3}{2})}{4\pi^2(d-2)^2} - \frac{(n-1)^2}{4\pi^2(d-2)} Y_0(\mu L) + \frac{n-1}{8\pi^2} Y_0(\mu L)^2 - \frac{(n-1)^2}{4\pi^2} Y_1(\mu L) \right) \right. \\
& \quad \left. + \left(-\frac{(n-1)^2}{2\pi(d-2)} + \frac{n-1}{2\pi} Y_0(\mu L) + \frac{(n-1)^2}{2\pi} (\ln \mu L) \right) \left(\frac{|\tau|}{L} \right) + \frac{(n-1)^2}{2} \left(\frac{|\tau|}{L} \right)^2 \right] \\
& + \mathcal{O}(g_{\text{MS}}^6) . \tag{A52}
\end{aligned}$$

In Eq. (A52), we abbreviate $\mathcal{O}((d-2)^2)$ terms in the coefficient of g_{MS}^2 , and $\mathcal{O}(d-2)$ terms in ones of g_{MS}^4 .

For the later discussion, we summarize the β function and the anomalous dimension. In general, the perturbative expression in R scheme can be written as

$$\beta_{\text{R}}(g_{\text{R}}^2) = (d-2) g_{\text{R}}^2 - g_{\text{R}}^4 \sum_{i=0}^{\infty} g_{\text{R}}^{2i} \beta_{\text{R},i} , \tag{A53}$$

$$\gamma_{\text{R}}(g_{\text{R}}^2) = -g_{\text{R}}^2 \sum_{i=0}^{\infty} g_{\text{R}}^{2i} \gamma_{\text{R},i} , \tag{A54}$$

with the dimensional regularization. For the MS scheme, each coefficient are given by

$$\beta_{\text{MS},0} = \frac{n-2}{2\pi} , \quad \beta_{\text{MS},1} = \frac{n-2}{4\pi^2} , \quad \beta_{\text{MS},2} = \frac{(n-2)(n+2)}{32\pi^3} , \tag{A55}$$

$$\gamma_{\text{MS},0} = -\frac{n-1}{2\pi} , \quad \gamma_{\text{MS},1} = 0 , \quad \gamma_{\text{MS},2} = -\frac{3(n-1)(n-2)}{32\pi^3} , \tag{A56}$$

up to the $\mathcal{O}(g_{\text{MS}}^6)$ order of the renormalization factor. $\beta_{\text{MS},2}$ and $\gamma_{\text{MS},2}$ have been first derived in Ref. [25]. The derivation is straightforward from Eqs. (A48), (A50) and (A51).

6. Renormalization in FV scheme

The zero-momentum projected $O(n)$ -invariant Green function can be re-expressed with the mass gap M and the amplitude A as

$$G_{\text{inv}}(x_0; y_0) |_{x_0=-\tau, y_0=+\tau} = A e^{-2|\tau|M} . \tag{A57}$$

Using the expansion

$$M = \sum_{i=1}^{\infty} g_{\text{MS}}^{2i} M_i, \quad A = 1 + \sum_{i=1}^{\infty} g_{\text{MS}}^{2i} A_i, \quad (\text{A58})$$

the right hand side of Eq. (A57) can be expand as

$$A e^{-2|\tau|M} = 1 + g_{\text{MS}}^2 \left[A_1 - 2LM_1 \left(\frac{|\tau|}{L} \right) \right] + g_{\text{MS}}^4 \left[A_2 - 2L(A_1 M_1 + M_2) \left(\frac{|\tau|}{L} \right) + 2L^2 M_1^2 \left(\frac{|\tau|}{L} \right)^2 \right] + \mathcal{O}(g_{\text{MS}}^6). \quad (\text{A59})$$

Comparing Eqs. (A52) and (A59), we obtain

$$M_1 = \frac{n-1}{2L} - \frac{(d-2)(n-1)}{2L} (\ln \mu L), \quad M_2 = \frac{(n-1)(n-2)}{2L} \times \frac{1}{2\pi} Y_0(\mu L), \quad (\text{A60})$$

$$A_1 = \frac{n-1}{2\pi(d-2)} - \frac{n-1}{2\pi} Y_0(\mu L) - \frac{(d-2)(n-1)}{2\pi} Y_1(\mu L),$$

$$A_2 = \frac{(n-1)(n-\frac{3}{2})}{4\pi^2(d-2)^2} - \frac{(n-1)^2}{4\pi^2(d-2)} Y_0(\mu L) + \frac{n-1}{8\pi^2} Y_0(\mu L)^2 - \frac{(n-1)^2}{4\pi^2} Y_1(\mu L). \quad (\text{A61})$$

We abbreviate $\mathcal{O}((d-2)^2)$ terms in M_1 and A_1 , and $\mathcal{O}(d-2)$ terms in M_2 and A_2 .

Until now, the perturbative evaluation of the mass gap in a finite box has been given at the $\mathcal{O}(g_{\text{MS}}^4)$ order [13, 16], the $\mathcal{O}(g_{\text{MS}}^6)$ order [2, 15, 19], and the $\mathcal{O}(g_{\text{MS}}^8)$ order [17]. The $\mathcal{O}(g_{\text{MS}}^6)$ expression is

$$M = \frac{n-1}{2L} [g_{\text{MS}}^2 + g_{\text{MS}}^4 C_1 + g_{\text{MS}}^6 C_2 + \mathcal{O}(g_{\text{MS}}^8)] , \quad (\text{A62})$$

with

$$C_1 = \frac{n-2}{2\pi} Y_0(\mu L), \quad C_2 = C_1^2 + \frac{C_1}{2\pi} + \frac{3(n-2)}{16\pi^2}. \quad (\text{A63})$$

Our evaluation in Eq. (A60) is consistent with C_1 in Eq. (A63) at $d = 2$.

The mass gap M does not depend on arbitrarily introduced μ . This fact means that the μ -dependence in C_i cancels with one in g_{MS}^2 , and M leaves only the L -dependence. The situation is same for the amplitude A .

We introduce the FV scheme. The μ - and L -dependences in each coefficient C_i appear only through the form of μL even in a higher order. Thus, if we set the renormalization scale by $\mu = 1/L$, the coefficient $c_i \equiv C_i|_{\mu=1/L}$ is a constant independent of μ and L . Then, we can consider the new renormalized coupling

$$g_{\text{FV}}^2 = g_{\text{MS}}^2 \left(1 + \sum_{i=1}^{\infty} g_{\text{MS}}^{2i} c_i \right). \quad (\text{A64})$$

Moreover, with the another constant coefficient $a_i \equiv A_i|_{\mu=1/L}$, we can introduce the new wave-function renormalization

$$Z_{\text{FV}}^\phi = 1 + \sum_{i=1}^{\infty} g_{\text{MS}}^{2i} a_i. \quad (\text{A65})$$

These are nothing less than the renormalization in the FV scheme, which has been discussed in Sec. II B.

7. β function and anomalous dimension in FV scheme

We discuss the β function and the anomalous dimension in the FV scheme. The β function in the FV scheme is converted from one in the MS scheme by

$$\beta_{\text{FV}}(g_{\text{FV}}^2) = \beta_{\text{MS}}(g_{\text{MS}}^2) \frac{dg_{\text{FV}}^2}{dg_{\text{MS}}^2} . \quad (\text{A66})$$

Substituting Eqs. (A53) and (A64) to Eq. (A66), at $d = 2$, we obtain

$$\beta_{\text{FV},0} = \beta_{\text{MS},0} , \quad \beta_{\text{FV},1} = \beta_{\text{MS},1} , \quad \beta_{\text{FV},2} = \beta_{\text{MS},2} - \beta_{\text{MS},1} c_1 - \beta_{\text{MS},0} (c_2 - c_1^2) , \quad (\text{A67})$$

up to the $\mathcal{O}(g_{\text{MS}}^6)$ of the renormalization factor. Then, we have

$$\beta_{\text{FV},0} = \frac{n-2}{2\pi} , \quad \beta_{\text{FV},1} = \frac{n-2}{4\pi^2} , \quad \beta_{\text{FV},2} = \frac{(n-1)(n-2)}{8\pi^3} . \quad (\text{A68})$$

with Eqs. (A55) and (A63). We add Eq. (A68) has been first given in Ref. [2].

The anomalous dimension in the FV scheme is converted from one in the MS scheme by

$$\gamma_{\text{FV}}(g_{\text{FV}}^2) = \gamma_{\text{MS}}(g_{\text{MS}}^2) + \beta_{\text{MS}}(g_{\text{MS}}^2) \frac{d}{dg_{\text{MS}}^2} \ln \eta(g_{\text{MS}}^2) \quad (\text{A69})$$

with $\eta \equiv Z_{\text{FV}}^\phi / Z_{\text{MS}}^\phi$. The difference of the renormalization scheme affects only the finite part. Thus, in the expansion of

$$\eta = 1 + \sum_{i=1}^{\infty} g_{\text{MS}}^{2i} \eta_i , \quad (\text{A70})$$

each coefficient η_i has no pole terms at $d = 2$. In fact, the coefficients are

$$\eta_1 = -\frac{n-1}{2\pi} (X_0 - 1) , \quad \eta_2 = \frac{n-1}{8\pi^2} (X_0 - 1)^2 , \quad (\text{A71})$$

up to $\mathcal{O}(g_{\text{MS}}^4)$ from Eqs. (A51) and (A65). Substituting Eqs. (A53), (A54), (A64) and (A70) to Eq. (A69), we obtain

$$\begin{aligned} \gamma_{\text{FV},0} &= \gamma_{\text{MS},0} , \quad \gamma_{\text{FV},1} = \gamma_{\text{MS},1} - \gamma_{\text{MS},0} c_1 + \beta_{\text{MS},0} \eta_1 , \\ \gamma_{\text{FV},2} &= \gamma_{\text{MS},2} - 2\gamma_{\text{MS},1} c_1 - \gamma_{\text{MS},0} (c_2 - 2c_1^2) + \beta_{\text{MS},1} \eta_1 + \beta_{\text{MS},0} (2\eta_2 - \eta_1^2 - 2\eta_1 c_1) , \end{aligned} \quad (\text{A72})$$

up to the $\mathcal{O}(g_{\text{MS}}^6)$ of the renormalization factor. Then, we have

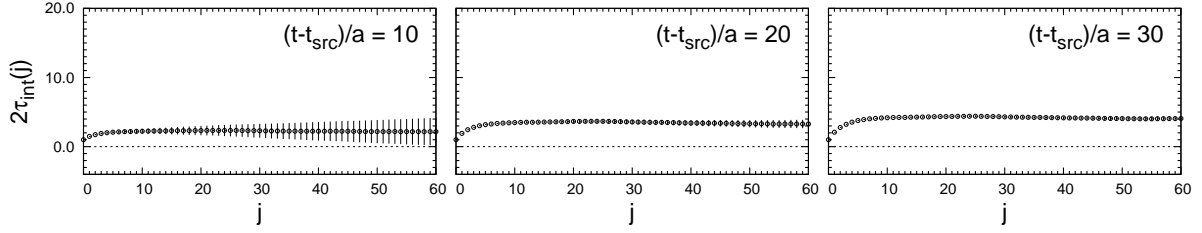
$$\gamma_{\text{FV},0} = -\frac{n-1}{2\pi} , \quad \gamma_{\text{FV},1} = 0 , \quad \gamma_{\text{FV},2} = 0 . \quad (\text{A73})$$

with Eqs. (A55), (A56), (A63) and (A71).

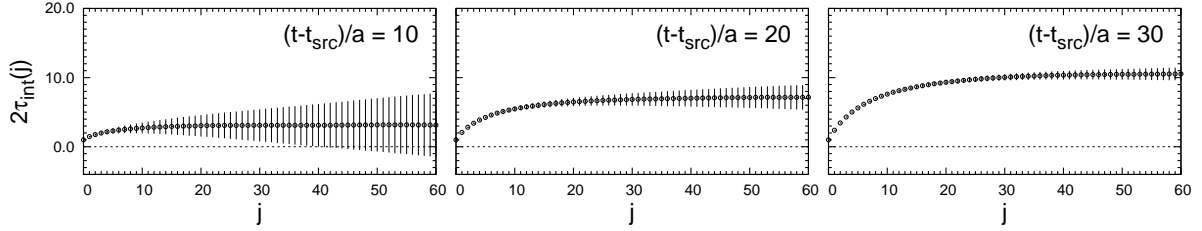
-
- [1] M. Lüscher, Commun. Math. Phys. **105** (1986) 153; Nucl. Phys. B **354** (1991) 531.
 - [2] M. Lüscher, P. Weisz and U. Wolff, Nucl. Phys. B **359** (1991) 221.
 - [3] V. Efimov, Phys. Lett. **33B** (1970) 563.
 - [4] M. Gell-Mann and M. Levy, Nuovo Cim. **16** (1960) 705.
 - [5] A. M. Polyakov, Phys. Lett. **59B** (1975) 79.
 - [6] A. A. Migdal, Sov. Phys. JETP **42** (1975) 743.
 - [7] E. Brézin and J. Zinn-Justin, Phys. Rev. Lett. **36** (1976) 691; Phys. Rev. B **14** (1976) 3110.
 - [8] E. Brézin, J. Zinn-Justin and J. C. Le Guillou, Phys. Rev. D **14** (1976) 2615.
 - [9] G. 't Hooft, Nucl. Phys. B **61** (1973) 455.
 - [10] N. D. Mermin and H. Wagner, Phys. Rev. Lett. **17** (1966) 1133.
 - [11] S. Elitzur, Nucl. Phys. B **212** (1983) 501.
 - [12] F. David, Commun. Math. Phys. **81** (1981) 149.
 - [13] M. Lüscher, Phys. Lett. **118B** (1982) 391.
 - [14] P. Hasenfratz, Phys. Lett. **141B** (1984) 385.
 - [15] E. G. Floratos and D. Petcher, Nucl. Phys. B **252** (1985) 689.
 - [16] E. Brézin and J. Zinn-Justin, Nucl. Phys. B **257** (1985) 867.
 - [17] D. S. Shin, Nucl. Phys. B **496** (1997) 408.
 - [18] F. Niedermayer and C. Weiermann, Nucl. Phys. B **842** (2011) 248.
 - [19] F. Niedermayer and P. Weisz, JHEP **1604** (2016) 110.
 - [20] F. Niedermayer and P. Weisz, JHEP **1606** (2016) 102.
 - [21] S. Capitani, M. Lüscher, R. Sommer and H. Wittig, Nucl. Phys. B **544** (1999) 669, Erratum:
[Nucl. Phys. B **582** (2000) 762]
 - [22] S. Calle Jimenez, M. Oka and K. Sasaki, in progress.
 - [23] P. Hasenfratz and H. Leutwyler, Nucl. Phys. B **343** (1990) 241.
 - [24] J. Zinn-Justin, Quantum Field Theory and Critical Phenomena, Fourth Edition (Clarendon Press, Oxford, 2002).
 - [25] S. Hikami and E. Brézin, J. Phys. A **11** (1978) 1141.

Figures

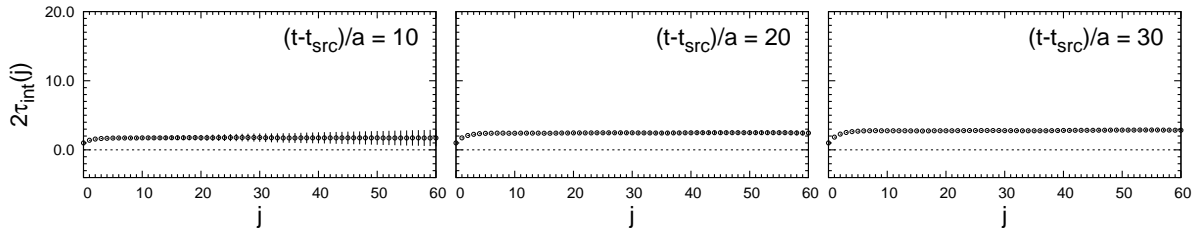
$$1/g^2 = 2.2403, L/a = 16$$



$$1/g^2 = 2.2403, L/a = 32$$



$$1/g^2 = 1.7800, L/a = 16$$



$$1/g^2 = 1.7800, L/a = 32$$

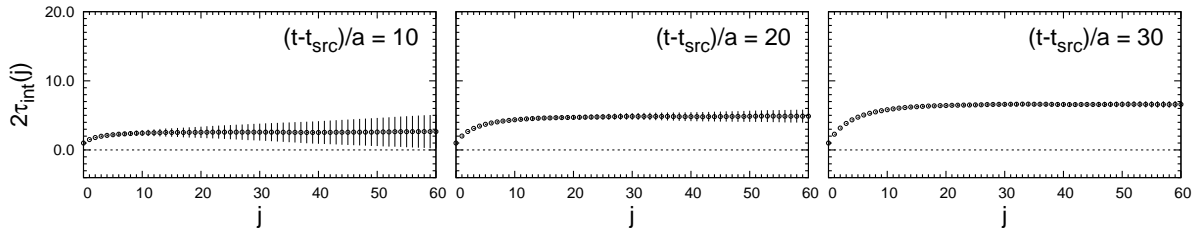


FIG. 1: $2\tau_{\text{int}}(j)$ for some $(1/g^2, L/a)$'s. We show the data for $1/g^2$ which give the smallest lattice spacing from the sets A and E. For each $(1/g^2, L/a)$, the situations with $(t - t_{\text{src}})/a = 10, 20$ and 30 are shown.

$$1/g^2 = 2.2403, \quad L/a = 32$$

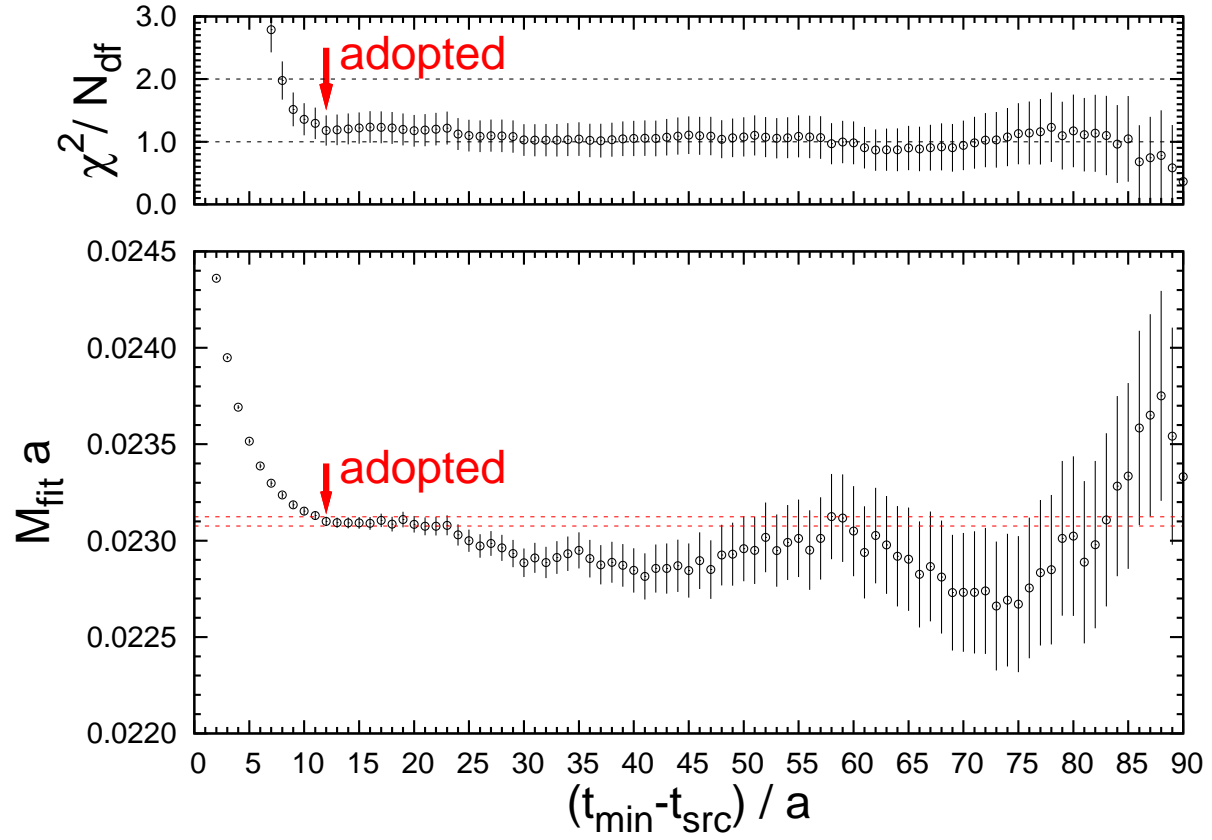


FIG. 2: An example of the fit-range dependence. χ^2/N_{df} in the fit is shown in the top panel, and the fitted mass gap, $M_{\text{fit}}a$, is in the bottom panel. For this parameter set, $(t_{\min} - t_{\text{src}})/a = 12$ is adopted.

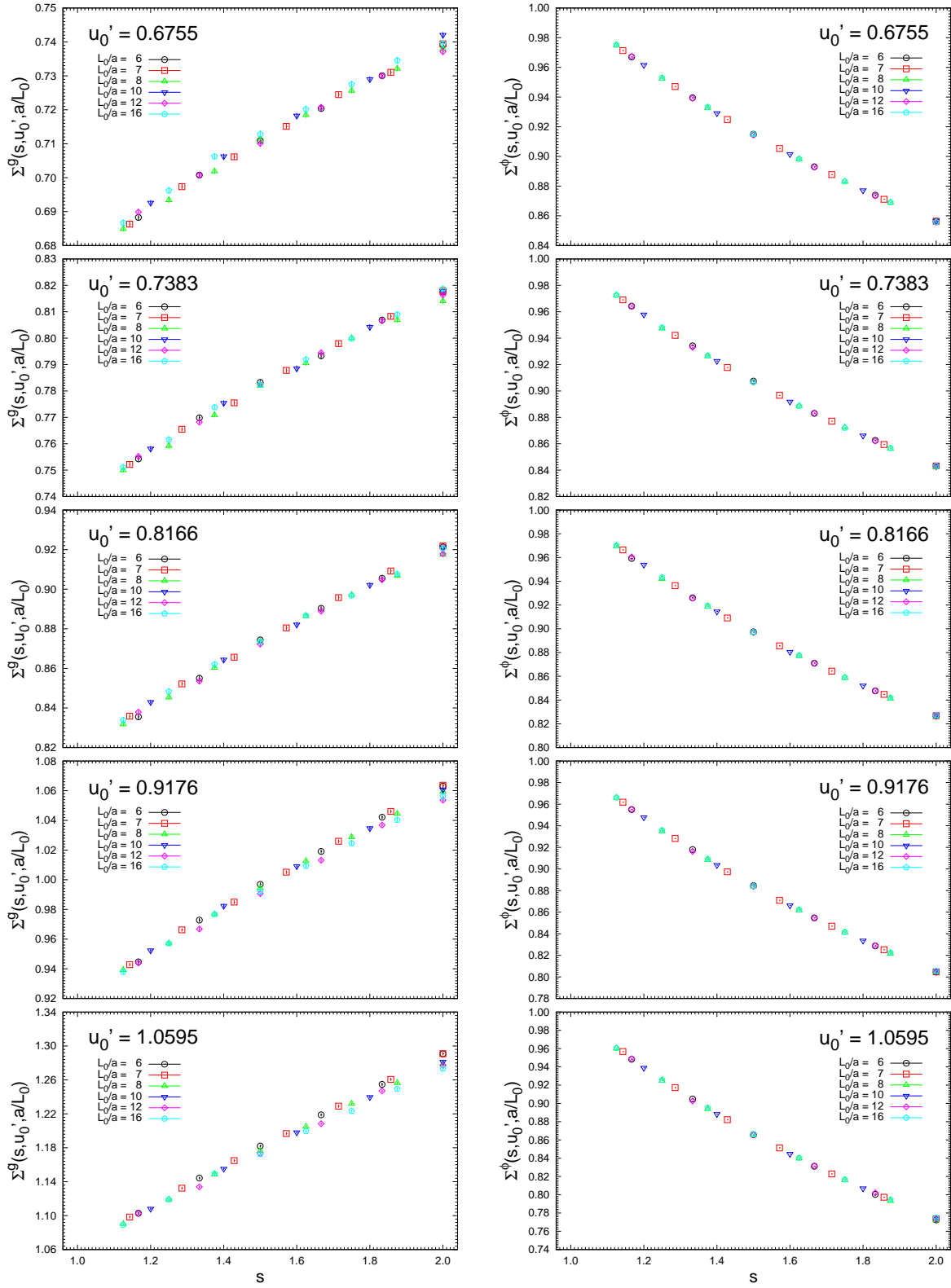


FIG. 3: s -dependence of $\Sigma^g(s, u'_0, a/L_0)$ and $\Sigma^\phi(s, u'_0, a/L_0)$ for various $(u'_0, L_0/a)$.

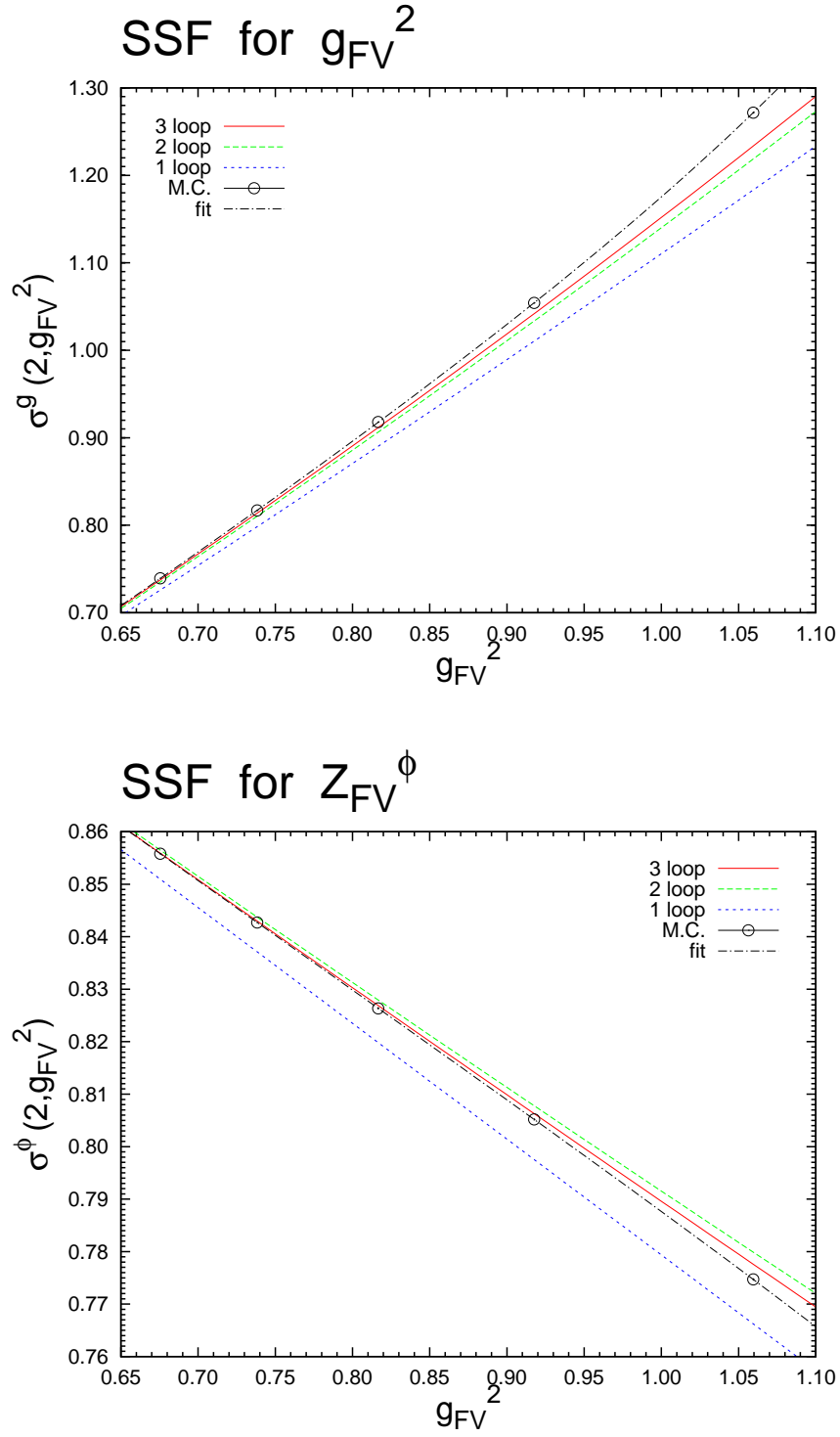


FIG. 4: SSFs obtained from the Monte Carlo simulation and perturbative evaluation. $\sigma^g(2, g_{FV}^2)$ is shown in the top panel, and $\sigma^\phi(2, g_{FV}^2)$ in the bottom panel. The 1-loop evaluation is described by the blue dotted curve, the 2-loop one by the green dashed curve, and the 3-loop one by the red solid curve. The result fitted to Eqs. (46) or (47) is given by the black dashed-dotted curve.

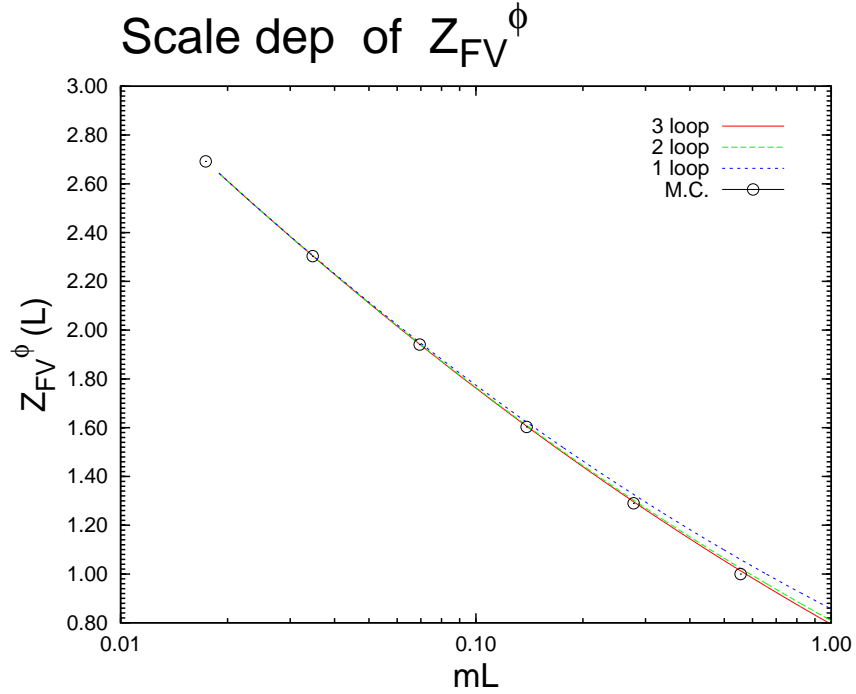
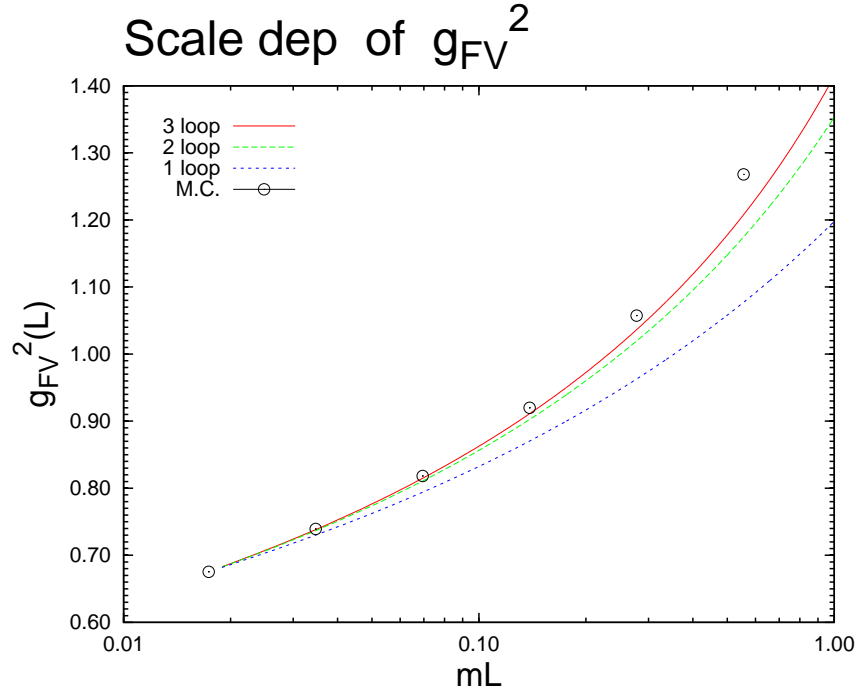


FIG. 5: Scale dependence of g_{FV}^2 and Z_{FV}^ϕ . In addition to the results by the Monte Carlo simulation, we also plot the results obtained by numerically integrating Eqs. (13) and (14) from $mL = 0.017366$ with the perturbative $\beta_{\text{FV}}(g_{\text{FV}}^2)$ and $\gamma_{\text{FV}}(g_{\text{FV}}^2)$. The 1-loop evaluation is described by the blue dotted curve, the 2-loop one by the green dashed curve, and the 3-loop one by the red solid curve.

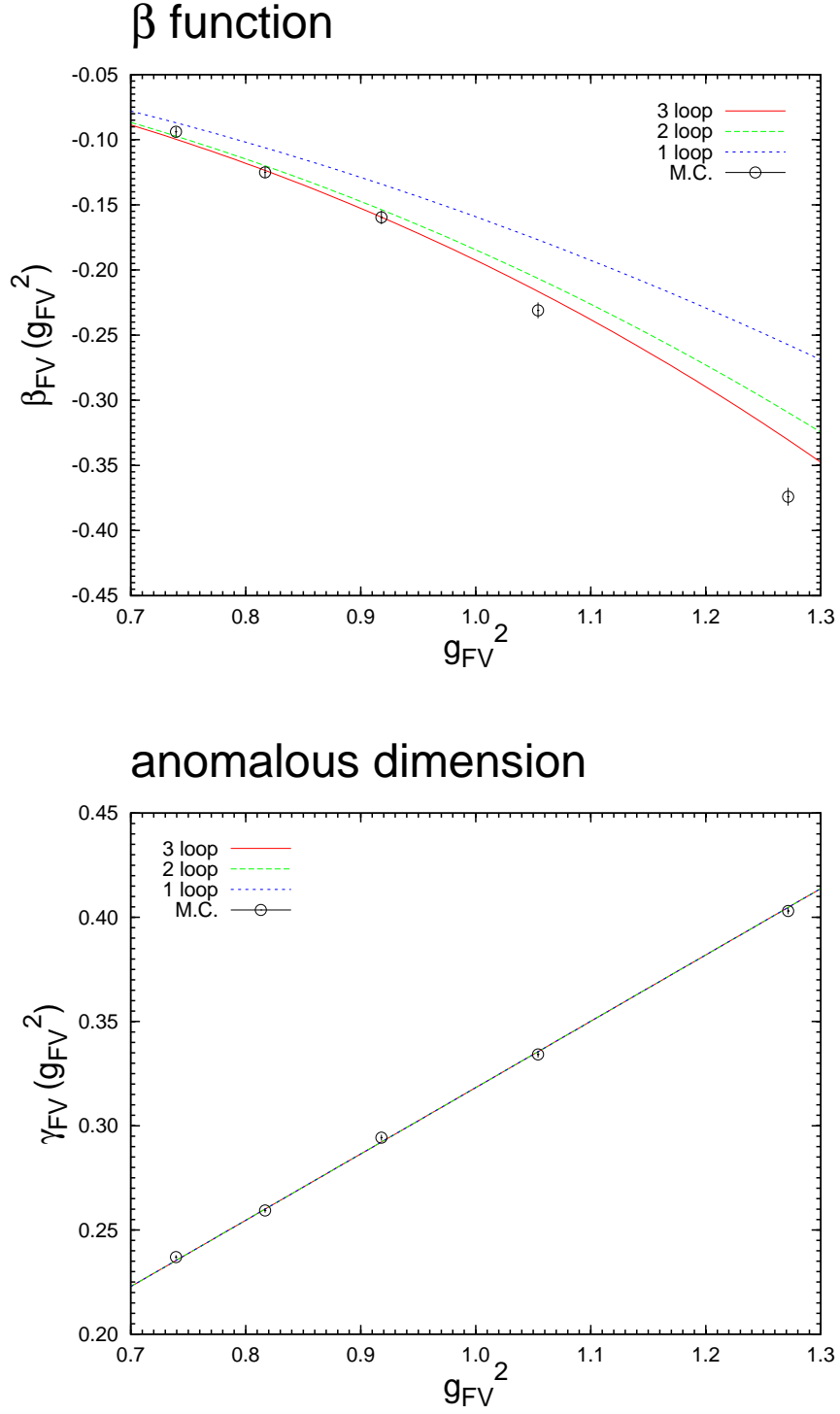


FIG. 6: $\beta_{FV}(\sigma^g(2, u'_0))$ and $\gamma_{FV}(\sigma^g(2, u'_0))$ determined in Sec. IV B. The former is shown in the top panel, and the latter in the bottom panel. The perturbative evaluation is also plotted for a comparison. The 1-loop evaluation is described by the blue dotted curve, the 2-loop one by the green dashed curve, and the 3-loop one by the red solid curve.

Feynman rules

propagator

$$(x,i) \text{ --- } (y,j) = \delta_{ij} G(x;y)$$

vertices

$$(x,i) \text{ --- } \times \text{ --- } (x,j) = \frac{(n-1)g^2}{2TL^{d-1}} \delta_{ij}$$

$$\begin{array}{l} (x^1,i^1) \\ (x^2,i^2) \end{array} \text{ --- } \bullet \text{ --- } \bullet \text{ --- } \begin{array}{l} (x^3,i^3) \\ (x^4,i^4) \end{array} = \frac{g^2}{8} \delta_{i^1 i^2} \delta_{i^3 i^4} [\partial_\mu^1 \partial_\mu^3 + \partial_\mu^1 \partial_\mu^4 + \partial_\mu^2 \partial_\mu^3 + \partial_\mu^2 \partial_\mu^4]_{x^1=x^2=x^3=x^4}$$

FIG. 7: Feynman rules read off from the action (A7) up to $\mathcal{O}(g^2)$. The x and y represent the coordinate. The i and j do the number of component for the π field. The cross symbol denotes a vertex due to the zero mode. The filled circle does a vertex due to the term $\frac{g^2}{8} \frac{(\partial_\mu \pi^2)^2}{1 - g^2 \pi^2}$. The dotted lines means that vertices linked by them are located at the same coordinate.

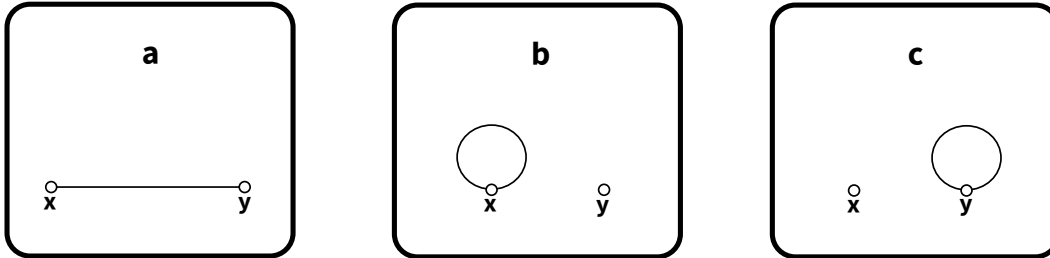


FIG. 8: The diagrammatic description of the $O(n)$ -invariant 2-point Green function at $\mathcal{O}(g^2)$. The open circle means the external space-time point.

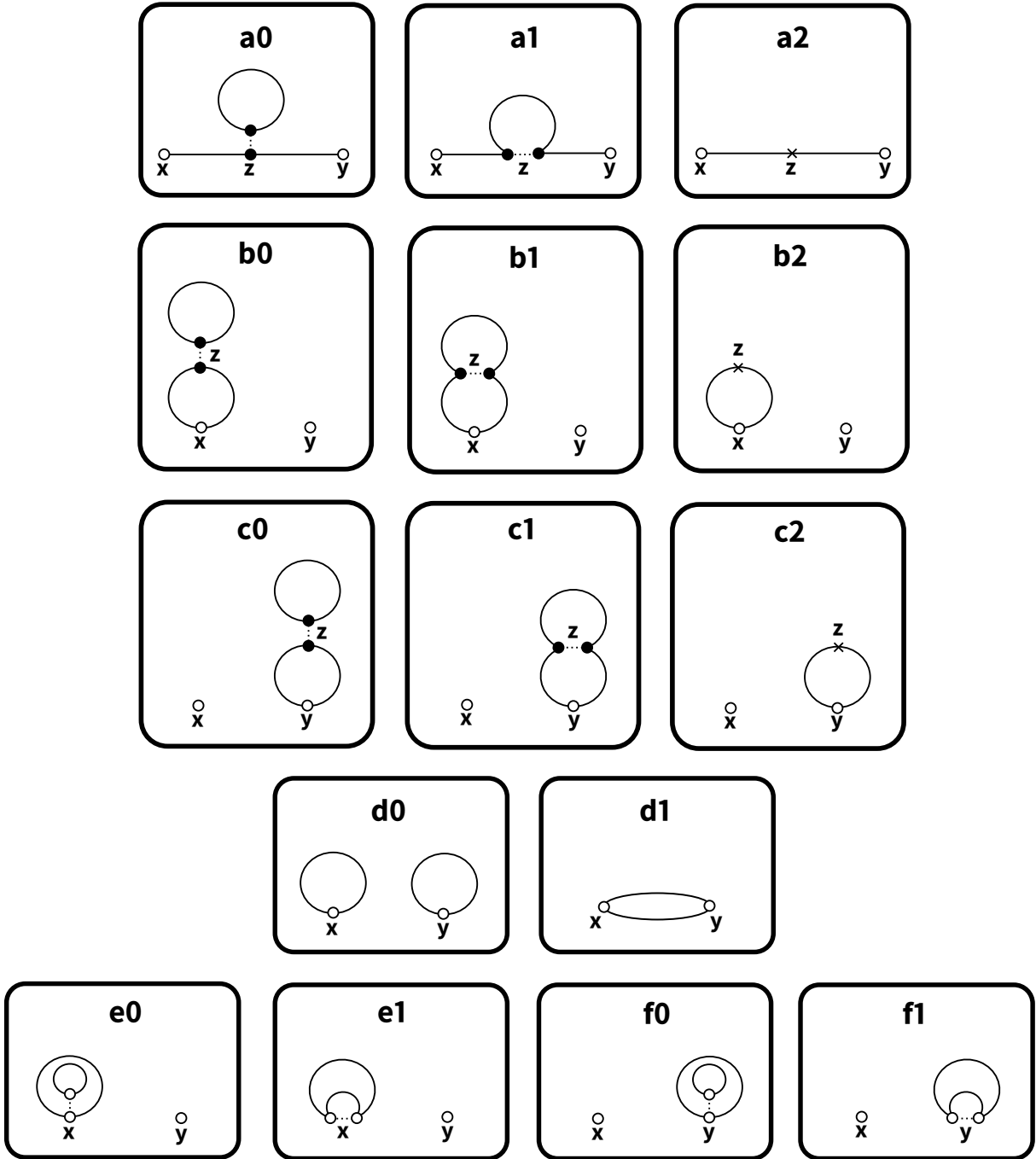


FIG. 9: The diagrammatic description of the $O(n)$ -invariant 2-point Green function at $\mathcal{O}(g^4)$.

Tables

TABLE I: A list of $(1/g^2, L/a)$ which are used in the present calculation.

set	$1/g^2$	L/a
A	2.0786	6, 7, 8, 9, 10, 11, 12
	2.1043	7, 8, 9, 10, 11, 12, 13, 14
	2.1275	8, 9, 10, 11, 12, 13, 14, 15, 16
	2.1625	10, 12, 14, 16, 18, 20
	2.1954	12, 14, 16, 18, 20, 22, 24
	2.2403	16, 18, 20, 22, 24, 26, 28, 30, 32
B	1.9637	6, 7, 8, 9, 10, 11, 12
	1.9875	7, 8, 9, 10, 11, 12, 13, 14
	2.0100	8, 9, 10, 11, 12, 13, 14, 15, 16
	2.0489	10, 12, 14, 16, 18, 20
	2.0794	12, 14, 16, 18, 20, 22, 24
	2.1260	16, 18, 20, 22, 24, 26, 28, 30, 32
C	1.8439	6, 7, 8, 9, 10, 11, 12
	1.8711	7, 8, 9, 10, 11, 12, 13, 14
	1.8947	8, 9, 10, 11, 12, 13, 14, 15, 16
	1.9319	10, 12, 14, 16, 18, 20
	1.9637	12, 14, 16, 18, 20, 22, 24
	2.0100	16, 18, 20, 22, 24, 26, 28, 30, 32
D	1.7276	6, 7, 8, 9, 10, 11, 12
	1.7553	7, 8, 9, 10, 11, 12, 13, 14
	1.7791	8, 9, 10, 11, 12, 13, 14, 15, 16
	1.8171	10, 12, 14, 16, 18, 20
	1.8497	12, 14, 16, 18, 20, 22, 24
	1.8965	16, 18, 20, 22, 24, 26, 28, 30, 32
E	1.6050	6, 7, 8, 9, 10, 11, 12
	1.6346	7, 8, 9, 10, 11, 12, 13, 14
	1.6589	8, 9, 10, 11, 12, 13, 14, 15, 16
	1.6982	10, 12, 14, 16, 18, 20
	1.7306	12, 14, 16, 18, 20, 22, 24
	1.7800	16, 18, 20, 22, 24, 26, 28, 30, 32

TABLE II: $g_{\text{FV}}^2(L, L/a)$ and $Z_{\text{FV}}^\phi(L, L/a)$ for various $(1/g^2, L/a)$ of set A.

$1/g^2 = 2.0786$				$1/g^2 = 2.1043$			
L/a	g_{FV}^2	Z_{FV}^ϕ	χ^2/N_{df}	L/a	g_{FV}^2	Z_{FV}^ϕ	χ^2/N_{df}
6	0.67562(44)	0.736987(89)	0.90(51)	7	0.67546(52)	0.71670(12)	0.83(45)
7	0.68841(53)	0.71269(12)	0.92(48)	8	0.68627(72)	0.69617(22)	1.92(67)
8	0.70089(50)	0.692435(98)	1.11(48)	9	0.69730(46)	0.678804(79)	1.06(44)
9	0.71109(47)	0.674314(80)	1.03(43)	10	0.70611(53)	0.66287(10)	1.00(41)
10	0.72053(54)	0.65817(10)	1.04(42)	11	0.71506(51)	0.648882(87)	1.38(45)

11	0.73019(52)	0.644050(89)	0.97(38)	12	0.72442(49)	0.636262(75)	0.81(33)
12	0.73917(59)	0.63109(11)	0.58(28)	13	0.73101(56)	0.624345(94)	0.85(33)
				14	0.73940(54)	0.613753(83)	0.98(33)
$1/g^2 = 2.1275$				$1/g^2 = 2.1625$			
L/a	g_{FV}^2	Z_{FV}^ϕ	χ^2/N_{df}	L/a	g_{FV}^2	Z_{FV}^ϕ	χ^2/N_{df}
8	0.67564(48)	0.700346(95)	1.30(52)	10	0.67532(50)	0.672916(98)	0.94(40)
9	0.68502(45)	0.682692(78)	1.18(46)	12	0.69241(47)	0.647087(74)	0.54(27)
10	0.69352(52)	0.66698(10)	1.08(42)	14	0.70607(51)	0.625249(80)	1.41(40)
11	0.70200(50)	0.653087(87)	1.63(49)	16	0.71807(48)	0.606667(65)	1.49(38)
12	0.71110(48)	0.640655(75)	0.59(28)	18	0.72879(61)	0.590271(93)	0.68(25)
13	0.71862(55)	0.629024(93)	1.09(37)	20	0.74184(51)	0.576403(61)	1.44(33)
14	0.72579(53)	0.618446(82)	1.01(34)				
15	0.73228(51)	0.608579(73)	0.96(32)				
16	0.73815(50)	0.599474(67)	1.29(36)				
$1/g^2 = 2.1954$				$1/g^2 = 2.2403$			
L/a	g_{FV}^2	Z_{FV}^ϕ	χ^2/N_{df}	L/a	g_{FV}^2	Z_{FV}^ϕ	χ^2/N_{df}
12	0.67551(46)	0.652903(72)	0.55(27)	16	0.67526(68)	0.62115(14)	1.11(34)
14	0.68986(43)	0.631629(58)	1.02(34)	18	0.68645(58)	0.605781(89)	0.65(24)
16	0.70072(47)	0.613205(64)	2.01(44)	20	0.69597(62)	0.591990(94)	0.99(28)
18	0.71007(60)	0.597037(92)	0.75(26)	22	0.70598(53)	0.579779(65)	1.25(30)
20	0.72075(64)	0.582953(96)	0.85(26)	24	0.71253(64)	0.568376(86)	1.08(27)
22	0.73000(62)	0.570317(82)	0.97(26)	26	0.71991(62)	0.558049(75)	0.90(23)
24	0.73715(74)	0.55872(11)	0.91(25)	28	0.72725(74)	0.548606(95)	0.82(22)
				30	0.73428(72)	0.539910(85)	1.17(25)
				32	0.73919(76)	0.531715(89)	1.18(24)

TABLE III: $g_{\text{FV}}^2(L, L/a)$ and $Z_{\text{FV}}^\phi(L, L/a)$ for various $(1/g^2, L/a)$ of set B.

$1/g^2 = 1.9637$				$1/g^2 = 1.9875$			
L/a	g_{FV}^2	Z_{FV}^ϕ	χ^2/N_{df}	L/a	g_{FV}^2	Z_{FV}^ϕ	χ^2/N_{df}
6	0.73747(63)	0.71909(17)	0.54(41)	7	0.73929(57)	0.69777(13)	1.12(53)
7	0.75339(58)	0.69344(13)	0.50(35)	8	0.75316(65)	0.67613(16)	0.96(46)
8	0.76891(55)	0.67183(10)	0.82(42)	9	0.76653(51)	0.657341(85)	1.56(53)
9	0.78230(52)	0.652625(87)	0.77(37)	10	0.77661(58)	0.64026(11)	0.80(36)
10	0.79236(71)	0.63504(16)	0.80(37)	11	0.78893(56)	0.625564(94)	0.77(34)
11	0.80587(57)	0.620335(95)	1.45(46)	12	0.79912(64)	0.61190(11)	0.79(33)
12	0.81642(66)	0.60642(12)	0.75(32)	13	0.80946(62)	0.59952(10)	1.05(36)
				14	0.81904(60)	0.588191(89)	0.97(33)
$1/g^2 = 2.0100$				$1/g^2 = 2.0489$			
L/a	g_{FV}^2	Z_{FV}^ϕ	χ^2/N_{df}	L/a	g_{FV}^2	Z_{FV}^ϕ	χ^2/N_{df}
8	0.74019(53)	0.68055(10)	1.29(52)	10	0.73761(66)	0.65247(15)	0.72(35)

9	0.75190(49)	0.661754(84)	0.79(38)	12	0.75740(60)	0.62503(11)	0.76(33)
10	0.76117(68)	0.64466(16)	0.58(32)	14	0.77468(57)	0.602081(86)	1.23(38)
11	0.77292(55)	0.630250(92)	1.07(40)	16	0.78772(80)	0.58195(15)	0.74(28)
12	0.78414(53)	0.616994(80)	0.80(33)	18	0.80339(68)	0.565226(98)	0.87(28)
13	0.79270(60)	0.604552(99)	0.82(32)	20	0.81694(73)	0.55012(10)	1.08(30)
14	0.80228(59)	0.593399(88)	1.30(39)				
15	0.80917(76)	0.58254(14)	0.98(33)				
16	0.81636(83)	0.57284(16)	1.30(37)				
$1/g^2 = 2.0794$				$1/g^2 = 2.1260$			
L/a	g_{FV}^2	Z_{FV}^ϕ	χ^2/N_{df}	L/a	g_{FV}^2	Z_{FV}^ϕ	χ^2/N_{df}
12	0.73826(59)	0.63119(11)	0.55(28)	16	0.73845(58)	0.599035(88)	1.00(32)
14	0.75515(55)	0.608666(84)	0.95(33)	18	0.75124(63)	0.582660(95)	1.05(31)
16	0.76813(78)	0.58894(15)	0.94(32)	20	0.76170(67)	0.567950(98)	0.93(27)
18	0.78243(66)	0.572381(96)	0.80(27)	22	0.77400(66)	0.555121(85)	1.25(30)
20	0.79442(71)	0.55745(10)	1.05(29)	24	0.78255(78)	0.54314(11)	0.94(25)
22	0.80650(69)	0.544151(87)	1.02(27)	26	0.79209(76)	0.532309(95)	1.01(25)
24	0.81634(81)	0.53195(11)	0.75(23)	28	0.80000(90)	0.52232(12)	1.10(25)
				30	0.80918(87)	0.51320(11)	0.86(21)
				32	0.81889(84)	0.505102(95)	0.83(20)

TABLE IV: $g_{\text{FV}}^2(L, L/a)$ and $Z_{\text{FV}}^\phi(L, L/a)$ for various $(1/g^2, L/a)$ of set C.

$1/g^2 = 1.8439$				$1/g^2 = 1.8711$			
L/a	g_{FV}^2	Z_{FV}^ϕ	χ^2/N_{df}	L/a	g_{FV}^2	Z_{FV}^ϕ	χ^2/N_{df}
6	0.81779(72)	0.69774(19)	0.59(42)	7	0.81674(80)	0.67550(23)	0.67(42)
7	0.8368(10)	0.66928(36)	1.30(61)	8	0.83601(60)	0.65282(11)	1.14(49)
8	0.85636(91)	0.64610(27)	1.09(51)	9	0.85232(57)	0.632517(92)	0.70(36)
9	0.87577(58)	0.626062(94)	1.01(43)	10	0.86582(78)	0.61411(17)	1.05(43)
10	0.89178(68)	0.60762(12)	0.95(40)	11	0.88066(75)	0.59823(14)	0.72(33)
11	0.90702(65)	0.59134(10)	1.12(41)	12	0.89595(72)	0.58385(12)	0.56(28)
12	0.92297(74)	0.57669(13)	0.93(36)	13	0.90939(70)	0.57061(11)	0.73(30)
				14	0.92210(68)	0.558491(97)	1.06(35)
$1/g^2 = 1.8947$				$1/g^2 = 1.9319$			
L/a	g_{FV}^2	Z_{FV}^ϕ	χ^2/N_{df}	L/a	g_{FV}^2	Z_{FV}^ϕ	χ^2/N_{df}
8	0.81744(59)	0.65790(11)	0.93(44)	10	0.81599(74)	0.62809(17)	1.10(44)
9	0.83262(55)	0.637830(91)	1.01(43)	12	0.84231(67)	0.59917(12)	0.72(32)
10	0.84622(76)	0.61976(17)	0.84(38)	14	0.86368(73)	0.57445(12)	1.23(38)
11	0.86124(62)	0.60431(10)	1.22(43)	16	0.88138(89)	0.55311(16)	0.95(32)
12	0.87416(70)	0.58991(12)	0.81(33)	18	0.90137(76)	0.53532(11)	1.06(31)
13	0.88743(68)	0.57696(11)	1.15(38)	20	0.92031(82)	0.51936(11)	0.91(27)
14	0.89816(66)	0.564864(94)	1.02(34)				

15	0.90795(85)	0.55333(15)	1.00(33)
16	0.91855(93)	0.54310(17)	0.86(30)

$1/g^2 = 1.9637$				$1/g^2 = 2.0100$			
L/a	g_{FV}^2	Z_{FV}^ϕ	χ^2/N_{df}	L/a	g_{FV}^2	Z_{FV}^ϕ	χ^2/N_{df}
12	0.81642(66)	0.60642(12)	0.75(32)	16	0.81636(83)	0.57284(16)	1.30(37)
14	0.83773(61)	0.582484(90)	0.80(30)	18	0.83360(70)	0.55586(10)	0.76(26)
16	0.85333(86)	0.56138(16)	1.10(34)	20	0.84805(75)	0.54043(11)	0.82(26)
18	0.87205(73)	0.54388(10)	0.78(26)	22	0.86180(74)	0.526669(91)	1.21(29)
20	0.88871(80)	0.52819(11)	0.93(27)	24	0.87336(88)	0.51403(12)	1.00(26)
22	0.90454(77)	0.514099(93)	1.16(29)	26	0.88646(85)	0.50271(10)	0.95(24)
24	0.91761(93)	0.50112(12)	0.92(25)	28	0.8965(10)	0.49211(13)	1.17(26)
				30	0.90739(98)	0.48235(11)	0.87(21)
				32	0.92037(95)	0.47385(10)	0.92(21)

TABLE V: $g_{\text{FV}}^2(L, L/a)$ and $Z_{\text{FV}}^\phi(L, L/a)$ for various $(1/g^2, L/a)$ of set D.

$1/g^2 = 1.7276$				$1/g^2 = 1.7553$			
L/a	g_{FV}^2	Z_{FV}^ϕ	χ^2/N_{df}	L/a	g_{FV}^2	Z_{FV}^ϕ	χ^2/N_{df}
6	0.91813(82)	0.67343(21)	0.96(54)	7	0.91732(73)	0.65013(16)	1.76(66)
7	0.94527(76)	0.64314(16)	1.27(56)	8	0.94251(68)	0.62534(12)	0.88(43)
8	0.97343(71)	0.61815(13)	1.36(53)	9	0.96594(65)	0.60345(10)	1.01(43)
9	0.99753(66)	0.59562(10)	0.53(31)	10	0.98462(90)	0.58341(19)	0.99(42)
10	1.01974(78)	0.57552(13)	0.70(34)	11	1.00482(86)	0.56624(16)	1.17(42)
11	1.04285(76)	0.55802(11)	0.93(37)	12	1.02561(83)	0.55070(14)	0.92(36)
12	1.06385(86)	0.54171(14)	0.94(36)	13	1.0457(81)	0.53651(12)	0.84(32)
				14	1.06333(79)	0.52324(11)	1.90(47)

$1/g^2 = 1.7791$				$1/g^2 = 1.8171$			
L/a	g_{FV}^2	Z_{FV}^ϕ	χ^2/N_{df}	L/a	g_{FV}^2	Z_{FV}^ϕ	χ^2/N_{df}
8	0.91775(66)	0.63133(12)	1.10(48)	10	0.91626(83)	0.60044(18)	1.08(43)
9	0.93942(63)	0.609855(99)	0.89(40)	12	0.95094(77)	0.56913(13)	0.82(34)
10	0.95722(87)	0.59030(19)	1.00(42)	14	0.98082(97)	0.54265(18)	0.67(29)
11	0.97698(70)	0.57354(11)	0.97(38)	16	1.00748(80)	0.52021(11)	1.04(32)
12	0.99454(81)	0.55794(13)	0.84(34)	18	1.03295(88)	0.50068(11)	0.72(25)
13	1.01269(78)	0.54394(12)	1.15(38)	20	1.05874(95)	0.48347(12)	0.92(27)
14	1.02894(77)	0.53101(10)	1.38(40)				
15	1.04460(98)	0.51874(16)	1.07(34)				
16	1.05967(84)	0.50782(11)	1.00(32)				

$1/g^2 = 1.8497$				$1/g^2 = 1.8965$			
L/a	g_{FV}^2	Z_{FV}^ϕ	χ^2/N_{df}	L/a	g_{FV}^2	Z_{FV}^ϕ	χ^2/N_{df}
12	0.91781(74)	0.57834(13)	0.79(33)	16	0.91747(94)	0.54374(17)	1.39(38)
14	0.94411(69)	0.552425(97)	0.82(31)	18	0.93771(79)	0.52531(11)	0.85(28)

16	0.96708(99)	0.52991(18)	0.92(31)	20	0.95696(86)	0.50888(11)	1.23(31)
18	0.99091(83)	0.51113(11)	0.74(26)	22	0.97658(84)	0.494351(98)	1.14(29)
20	1.01343(91)	0.49428(12)	1.01(29)	24	0.9918(10)	0.48081(13)	0.88(24)
22	1.03716(89)	0.47935(10)	1.04(27)	26	1.00912(98)	0.46880(10)	1.03(25)
24	1.0539(11)	0.46540(13)	1.15(28)	28	1.0244(11)	0.45765(12)	0.90(23)
				30	1.0401(11)	0.44730(12)	1.05(24)
				32	1.0560(11)	0.43810(11)	1.47(27)

TABLE VI: $g_{\text{FV}}^2(L, L/a)$ and $Z_{\text{FV}}^\phi(L, L/a)$ for various $(1/g^2, L/a)$ of set E.

$1/g^2 = 1.6050$				$1/g^2 = 1.6346$			
L/a	g_{FV}^2	Z_{FV}^ϕ	χ^2/N_{df}	L/a	g_{FV}^2	Z_{FV}^ϕ	χ^2/N_{df}
6	1.05866(98)	0.64252(24)	1.58(70)	7	1.0574(11)	0.61760(29)	0.36(31)
7	1.10194(90)	0.60934(18)	1.16(54)	8	1.09602(81)	0.59098(14)	1.14(49)
8	1.14332(85)	0.58142(14)	1.78(61)	9	1.12986(76)	0.56664(11)	1.28(48)
9	1.18096(80)	0.55636(12)	0.64(34)	10	1.16218(90)	0.54500(15)	0.77(36)
10	1.21769(95)	0.53412(15)	1.12(43)	11	1.19398(87)	0.52598(13)	0.72(33)
11	1.2535(11)	0.51437(19)	0.72(33)	12	1.2261(10)	0.50844(16)	1.32(43)
12	1.2896(11)	0.49645(16)	1.37(44)	13	1.25752(99)	0.49268(14)	0.92(34)
				14	1.28756(97)	0.47814(12)	1.26(38)
$1/g^2 = 1.6589$				$1/g^2 = 1.6982$			
L/a	g_{FV}^2	Z_{FV}^ϕ	χ^2/N_{df}	L/a	g_{FV}^2	Z_{FV}^ϕ	χ^2/N_{df}
8	1.06073(78)	0.59846(13)	0.80(41)	10	1.05950(82)	0.56631(14)	0.78(36)
9	1.09148(73)	0.57462(11)	0.66(35)	12	1.10810(90)	0.53170(14)	1.42(44)
10	1.12050(87)	0.55344(14)	0.66(33)	14	1.15522(86)	0.50309(11)	0.65(27)
11	1.14998(84)	0.53491(12)	1.21(42)	16	1.19819(97)	0.47839(12)	1.19(35)
12	1.17791(97)	0.51778(15)	0.69(31)	18	1.2397(11)	0.45698(13)	0.91(29)
13	1.20647(94)	0.50241(13)	1.12(38)	20	1.2813(12)	1.43811(14)	0.90(27)
14	1.23363(92)	0.48817(12)	1.47(41)				
15	1.2582(12)	0.47455(19)	1.25(37)				
16	1.2810(14)	0.46181(22)	1.26(37)				
$1/g^2 = 1.7306$				$1/g^2 = 1.7800$			
L/a	g_{FV}^2	Z_{FV}^ϕ	χ^2/N_{df}	L/a	g_{FV}^2	Z_{FV}^ϕ	χ^2/N_{df}
12	1.05944(86)	0.54277(14)	0.86(35)	16	1.05797(84)	0.50805(11)	1.18(34)
14	1.10256(82)	0.51503(11)	0.84(31)	18	1.08760(93)	0.48799(12)	0.77(26)
16	1.1338(12)	0.48998(20)	0.70(27)	20	1.1172(10)	0.47038(13)	0.91(27)
18	1.1731(10)	0.46981(12)	1.09(31)	22	1.14777(87)	0.454904(84)	1.01(27)
20	1.2083(11)	0.45137(13)	0.99(28)	24	1.1707(12)	0.44014(14)	0.93(25)
22	1.2470(11)	0.43537(11)	0.75(23)	26	1.1976(12)	0.42709(12)	1.03(25)
24	1.2772(13)	0.42008(15)	0.92(25)	28	1.2213(13)	0.41507(13)	1.36(28)
				30	1.2472(12)	0.40391(11)	1.11(24)
				32	1.2712(13)	0.39383(12)	0.81(20)

TABLE VII: $\Sigma^g(s, u'_0, a/L_0)$ and $\Sigma^\phi(s, u'_0, a/L_0)$ for set A ($u'_0 = 0.6755$).

$L_0/a = 6$			$L_0/a = 7$		
s	Σ^g	Σ^ϕ	s	Σ^g	Σ^ϕ
7/6	0.68829(75)	0.96704(20)	8/7	0.68631(95)	0.97135(35)
8/6	0.70076(73)	0.93956(18)	9/7	0.69735(78)	0.94712(20)
9/6	0.71095(71)	0.91498(17)	10/7	0.70616(82)	0.92488(22)
10/6	0.72039(76)	0.89308(19)	11/7	0.71512(80)	0.90537(21)
11/6	0.73004(75)	0.87392(18)	12/7	0.72447(79)	0.88776(20)
12/6	0.73902(80)	0.85634(20)	13/7	0.73106(84)	0.87113(22)
			14/7	0.73945(83)	0.85635(21)
$L_0/a = 7$			$L_0/a = 10$		
s	Σ^g	Σ^ϕ	s	Σ^g	Σ^ϕ
9/8	0.68488(73)	0.97480(17)	12/10	0.69260(77)	0.96161(18)
10/8	0.69337(78)	0.95236(20)	14/10	0.70628(80)	0.92914(19)
11/8	0.70185(76)	0.93253(18)	16/10	0.71828(78)	0.90152(18)
12/8	0.71094(75)	0.91479(17)	18/10	0.72900(86)	0.87715(21)
13/8	0.71847(80)	0.89818(19)	20/10	0.74207(80)	0.85653(19)
14/8	0.72562(78)	0.88308(19)			
15/8	0.73212(77)	0.86900(18)			
16/8	0.73799(76)	0.85600(18)			
$L_0/a = 12$			$L_0/a = 16$		
s	Σ^g	Σ^ϕ	s	Σ^g	Σ^ϕ
14/12	0.68985(70)	0.96742(14)	18/16	0.6867(10)	0.97525(26)
16/12	0.70071(73)	0.93920(15)	20/16	0.6962(10)	0.95304(27)
18/12	0.71007(81)	0.91444(18)	22/16	0.70624(98)	0.93337(25)
20/12	0.72074(84)	0.89286(19)	24/16	0.7128(10)	0.91501(26)
22/12	0.73000(83)	0.87351(18)	26/16	0.7202(10)	0.89838(26)
24/12	0.73714(92)	0.85574(21)	28/16	0.7275(11)	0.88317(28)
			30/16	0.7346(11)	0.86917(27)
			32/16	0.7395(11)	0.85597(28)

TABLE VIII: $\Sigma^g(s, u'_0, a/L_0)$ and $\Sigma^\phi(s, u'_0, a/L_0)$ for set B ($u'_0 = 0.7383$).

$L_0/a = 6$			$L_0/a = 7$		
s	Σ^g	Σ^ϕ	s	Σ^g	Σ^ϕ
7/6	0.75426(98)	0.96428(30)	8/7	0.75214(96)	0.96903(29)
8/6	0.76981(96)	0.93420(28)	9/7	0.76547(86)	0.94215(22)
9/6	0.78323(94)	0.90746(26)	10/7	0.77552(91)	0.91770(24)

10/6	0.7933(11)	0.88298(33)	11/7	0.78780(90)	0.89666(23)
11/6	0.80687(97)	0.86251(28)	12/7	0.79796(95)	0.87710(25)
12/6	0.8175(10)	0.84313(30)	13/7	0.80826(93)	0.85938(24)
			14/7	0.81781(92)	0.84318(24)
$L_0/a = 8$			$L_0/a = 10$		
s	Σ^g	Σ^ϕ	s	Σ^g	Σ^ϕ
9/8	0.74995(81)	0.97245(19)	12/10	0.7581(10)	0.95790(28)
10/8	0.75916(94)	0.94738(27)	14/10	0.77545(99)	0.92270(26)
11/8	0.77085(85)	0.92627(20)	16/10	0.7885(11)	0.89182(33)
12/8	0.78200(84)	0.90685(19)	18/10	0.8042(11)	0.86616(28)
13/8	0.79052(88)	0.88861(21)	20/10	0.8178(11)	0.84299(29)
14/8	0.80004(87)	0.87227(20)			
15/8	0.80689(99)	0.85635(26)			
16/8	0.8140(11)	0.84212(28)			
$L_0/a = 12$			$L_0/a = 16$		
s	Σ^g	Σ^ϕ	s	Σ^g	Σ^ϕ
14/12	0.75519(91)	0.96431(21)	18/16	0.75109(95)	0.97267(21)
16/12	0.7682(11)	0.93305(29)	20/16	0.76155(97)	0.94812(22)
18/12	0.78247(98)	0.90682(23)	22/16	0.77384(97)	0.92671(21)
20/12	0.7945(10)	0.88316(24)	24/16	0.7824(11)	0.90672(24)
22/12	0.8065(10)	0.86210(23)	26/16	0.7919(10)	0.88863(22)
24/12	0.8164(11)	0.84277(26)	28/16	0.7998(11)	0.87196(26)
			30/16	0.8090(11)	0.85674(24)
			32/16	0.8187(11)	0.84323(24)

TABLE IX: $\Sigma^g(s, u'_0, a/L_0)$ and $\Sigma^\phi(s, u'_0, a/L_0)$ for set C ($u'_0 = 0.8166$).

$L_0/a = 6$			$L_0/a = 7$		
s	Σ^g	Σ^ϕ	s	Σ^g	Σ^ϕ
7/6	0.8355(13)	0.95926(58)	8/7	0.8359(12)	0.96644(37)
8/6	0.8550(13)	0.92610(47)	9/7	0.8522(12)	0.93639(35)
9/6	0.8744(11)	0.89743(30)	10/7	0.8657(13)	0.90914(41)
10/6	0.8903(11)	0.87103(32)	11/7	0.8805(13)	0.88563(39)
11/6	0.9055(11)	0.84774(31)	12/7	0.8958(12)	0.86435(37)
12/6	0.9214(12)	0.82678(33)	13/7	0.9092(12)	0.84476(37)
			14/7	0.9219(12)	0.82682(36)
$L_0/a = 8$			$L_0/a = 10$		
s	Σ^g	Σ^ϕ	s	Σ^g	Σ^ϕ
9/8	0.83175(92)	0.96953(21)	12/10	0.8430(12)	0.95392(32)
10/8	0.8453(11)	0.94209(30)	14/10	0.8644(12)	0.91453(32)
11/8	0.86030(97)	0.91863(22)	16/10	0.8821(13)	0.88053(37)

12/8	0.8732(10)	0.89678(25)	18/10	0.9021(12)	0.85218(31)
13/8	0.8864(10)	0.87710(24)	20/10	0.9211(12)	0.82675(33)
14/8	0.89713(99)	0.85874(23)			
15/8	0.9069(11)	0.84123(29)			
16/8	0.9175(12)	0.82569(32)			
$L_0/a = 12$			$L_0/a = 16$		
s	Σ^g	Σ^ϕ	s	Σ^g	Σ^ϕ
14/12	0.8379(10)	0.96052(24)	18/16	0.8338(13)	0.97034(32)
16/12	0.8535(12)	0.92571(32)	20/16	0.8483(13)	0.94341(32)
18/12	0.8723(11)	0.89685(26)	22/16	0.8621(13)	0.91937(31)
20/12	0.8889(12)	0.87096(27)	24/16	0.8736(14)	0.89731(34)
22/12	0.9048(11)	0.84773(26)	26/16	0.8867(14)	0.87753(33)
24/12	0.9178(12)	0.82632(29)	28/16	0.8967(15)	0.85903(36)
			30/16	0.9077(14)	0.84198(35)
			32/16	0.9207(14)	0.82714(34)

TABLE X: $\Sigma^g(s, u'_0, a/L_0)$ and $\Sigma^\phi(s, u'_0, a/L_0)$ for set D ($u'_0 = 0.9176$).

$L_0/a = 6$			$L_0/a = 7$		
s	Σ^g	Σ^ϕ	s	Σ^g	Σ^ϕ
7/6	0.9447(13)	0.95505(39)	8/7	0.9428(12)	0.96185(30)
8/6	0.9728(13)	0.91796(36)	9/7	0.9662(12)	0.92817(28)
9/6	0.9969(13)	0.88453(34)	10/7	0.9849(13)	0.89734(38)
10/6	1.0191(13)	0.85469(36)	11/7	1.0052(13)	0.87092(34)
11/6	1.0422(13)	0.82873(36)	12/7	1.0260(13)	0.84700(32)
12/6	1.0631(14)	0.80452(38)	13/7	1.0461(13)	0.82517(31)
			14/7	1.0637(12)	0.80476(30)
$L_0/a = 8$			$L_0/a = 10$		
s	Σ^g	Σ^ϕ	s	Σ^g	Σ^ϕ
9/8	0.9393(11)	0.96599(24)	12/10	0.9524(13)	0.94778(36)
10/8	0.9571(12)	0.93501(35)	14/10	0.9824(15)	0.90361(42)
11/8	0.9768(11)	0.90847(25)	16/10	1.0091(14)	0.86618(34)
12/8	0.9944(12)	0.88376(29)	18/10	1.0347(14)	0.83360(36)
13/8	1.0125(12)	0.86160(27)	20/10	1.0606(15)	0.80490(37)
14/8	1.0288(12)	0.84112(26)			
15/8	1.0444(13)	0.82170(33)			
16/8	1.0595(12)	0.80439(28)			
$L_0/a = 12$			$L_0/a = 16$		
s	Σ^g	Σ^ϕ	s	Σ^g	Σ^ϕ
14/12	0.9439(12)	0.95521(27)	18/16	0.9378(15)	0.96610(36)
16/12	0.9668(14)	0.91629(37)	20/16	0.9571(15)	0.93587(37)

18/12	0.9907(13)	0.88382(29)	22/16	0.9767(15)	0.90915(35)
20/12	1.0132(13)	0.85469(30)	24/16	0.9919(16)	0.88424(38)
22/12	1.0369(13)	0.82889(29)	26/16	1.0093(16)	0.86215(37)
24/12	1.0536(14)	0.80476(33)	28/16	1.0246(16)	0.84165(38)
			30/16	1.0403(17)	0.82261(39)
			32/16	1.0562(16)	0.80567(38)

TABLE XI: $\Sigma^g(s, u'_0, a/L_0)$ and $\Sigma^\phi(s, u'_0, a/L_0)$ for set E ($u'_0 = 1.0595$).

$L_0/a = 6$			$L_0/a = 7$		
s	Σ^g	Σ^ϕ	s	Σ^g	Σ^ϕ
7/6	1.1029(16)	0.94831(46)	8/7	1.0983(17)	0.95677(51)
8/6	1.1443(16)	0.90480(42)	9/7	1.1323(17)	0.91727(48)
9/6	1.1820(16)	0.86577(41)	10/7	1.1648(18)	0.88216(50)
10/6	1.2188(17)	0.83113(44)	11/7	1.1968(17)	0.85129(49)
11/6	1.2548(18)	0.80037(48)	12/7	1.2291(18)	0.82282(51)
12/6	1.2909(17)	0.77243(46)	13/7	1.2607(18)	0.79723(50)
			14/7	1.2909(18)	0.77363(50)
$L_0/a = 8$			$L_0/a = 10$		
s	Σ^g	Σ^ϕ	s	Σ^g	Σ^ϕ
9/8	1.0902(13)	0.96023(29)	12/10	1.1081(15)	0.93888(35)
10/8	1.1191(14)	0.92487(32)	14/10	1.1552(14)	0.88836(31)
11/8	1.1485(14)	0.89396(30)	16/10	1.1982(15)	0.84474(33)
12/8	1.1764(14)	0.86538(34)	18/10	1.2397(16)	0.80695(35)
13/8	1.2048(14)	0.83973(32)	20/10	1.2813(16)	0.77362(37)
14/8	1.2319(14)	0.81597(31)			
15/8	1.2564(16)	0.79323(40)			
16/8	1.2791(17)	0.77197(45)			
$L_0/a = 12$			$L_0/a = 16$		
s	Σ^g	Σ^ϕ	s	Σ^g	Σ^ϕ
14/12	1.1026(15)	0.94887(32)	18/16	1.0892(15)	0.96045(32)
16/12	1.1339(17)	0.90272(44)	20/16	1.1190(15)	0.92574(33)
18/12	1.1731(16)	0.86557(34)	22/16	1.1496(15)	0.89521(28)
20/12	1.2083(16)	0.83158(36)	24/16	1.1727(17)	0.86611(35)
22/12	1.2471(16)	0.80210(35)	26/16	1.1996(17)	0.84037(33)
24/12	1.2773(18)	0.77393(40)	28/16	1.2234(17)	0.81670(35)
			30/16	1.2494(17)	0.79469(34)
			32/16	1.2735(18)	0.77481(35)

TABLE XII: The fitting results to Eqs. (35) and (36) with $(i_{\max}, j_{\max}) = (2, 2)$. We show $\sigma^g(2, u'_0) = \Sigma^g(2, u'_0, 0)$ and $\sigma^\phi(2, u'_0) = \Sigma^\phi(2, u'_0, 0)$ for each u'_0 . We also list the β function and the anomalous dimension at $\sigma^g(2, u'_0) = \Sigma^g(2, u'_0, 0)$.

u'_0	0.6755	0.7383	0.8166	0.9176	1.0595
χ^2/N_{df} for Σ^g	1.57	1.20	1.15	1.33	1.60
χ^2/N_{df} for Σ^ϕ	1.33	1.69	2.07	1.31	2.18
$\sigma^g(2, u'_0)$	0.73932(59)	0.81688(68)	0.91793(83)	1.05414(95)	1.2716(11)
$\sigma^\phi(2, u'_0)$	0.85580(14)	0.84272(16)	0.82635(21)	0.80520(23)	0.77470(24)
$\beta_{\text{FV}}(\sigma^g(2, u'_0))$	-0.0939(37)	-0.1251(43)	-0.1595(53)	-0.2310(61)	-0.3741(69)
$\gamma_{\text{FV}}(\sigma^g(2, u'_0))$	0.23698(93)	0.2593(11)	0.2943(14)	0.3342(16)	0.4031(16)

TABLE XIII: $g_{\text{FV}}^2(2^k L_{\min})$ and $Z_{\text{FV}}^\phi(2^k L_{\min})$ ($k = 0, \dots, 5$) determined with the SSFs by using Eqs. (15) and (16). We set $g_{\text{FV}}^2(L_{\max}) = 1.2680$ and $Z_{\text{FV}}^\phi(L_{\max}) = 1.0$ without statistical errors at $L_{\max} = 2^5 L_{\min}$. $g_{\text{FV}}^2(L_{\max}) = 1.2680$ corresponds to $mL_{\max} = 0.5557(13)$.

k	$m \times 2^k L_{\min}$	$g_{\text{FV}}^2(2^k L_{\min})$	$Z_{\text{FV}}^\phi(2^k L_{\min})$
0	0.017366(41)	0.67548(76)	2.6916(13)
1	0.034731(81)	0.73917(74)	2.3035(11)
2	0.06946(16)	0.81829(80)	1.94076(87)
3	0.13893(33)	0.91982(81)	1.60311(66)
4	0.27785(65)	1.05738(63)	1.29005(39)
5	0.5557(13)	1.2680	1.0

TABLE XIV: The explicit forms of each $P(\tau)$ in Eq. (A33) and the factor to be multiplied F . The prime in $\sum'_{\mathbf{p}}$ means that the $\mathbf{p} = \mathbf{0}$ contribution is excluded from the summation. Note that $\frac{1}{2L^{d-1}} \left(\sum'_{\mathbf{p}} \frac{1}{\mathbf{p}^2} \right)$ is nothing less than $R(0)$.

diagram	$P(\tau)$	F
a0	$\frac{1}{L^{2(d-1)}} \left[\left(\frac{7\tau^4}{6T^2} - \frac{4\tau^3}{3T} + \frac{\tau^2}{12} + \frac{T^2}{1440} \right) + \left(\sum'_{\mathbf{p}} \frac{1}{\mathbf{p}^2} \right) \left(-\frac{\tau^2}{2T^2} + \frac{1}{24} \right) + \left(\sum'_{\mathbf{p}} \frac{1}{\mathbf{p}^4} \right) \left(-\frac{3}{4T^2} \right) \right]$	$-\frac{(n-1)^2 g^4}{2}$
a1	$\frac{1}{L^{2(d-1)}} \left[\left(\frac{5\tau^4}{6T^2} - \frac{\tau^3}{T} + \frac{5\tau^2}{12} - \frac{T\tau}{12} + \frac{11T^2}{1440} \right) + \left(\sum'_{\mathbf{p}} \frac{1}{ \mathbf{p} } \right) \left(\frac{\tau^2}{2T} - \frac{\tau}{2} + \frac{T}{24} \right) + \left(\sum'_{\mathbf{p}} \frac{1}{\mathbf{p}^4} \right) \left(\frac{1}{4T^2} \right) \right]$	$-(n-1)g^4$
a2	$\frac{1}{L^{d-1}} \left(-\frac{\tau^4}{3T} + \frac{2\tau^3}{3} - \frac{T\tau^2}{3} + \frac{T^3}{720} \right)$	$-\frac{(n-1)^2 g^4}{TL^{d-1}}$
b0	$\frac{1}{L^{2(d-1)}} \left[\left(\frac{7\tau^4}{6T^2} + \frac{\tau^2}{12} + \frac{T^2}{1440} \right) + \left(\sum'_{\mathbf{p}} \frac{1}{\mathbf{p}^2} \right) \left(-\frac{\tau^2}{2T^2} + \frac{1}{24} \right) + \left(\sum'_{\mathbf{p}} \frac{1}{ \mathbf{p} ^3} \right) \left(-\frac{1}{2T} \right) + \left(\sum'_{\mathbf{p}} \frac{1}{\mathbf{p}^4} \right) \left(-\frac{3}{4T^2} \right) \right]$	$+\frac{(n-1)^2 g^4}{4}$

b1	$\frac{1}{L^{2(d-1)}} \left[\left(\frac{5\tau^4}{6T^2} - \frac{\tau^2}{12} + \frac{11T^2}{1440} \right) + \left(\sum_{\mathbf{p}}' \frac{1}{ \mathbf{p} } \right) \left(\frac{\tau^2}{T} + \frac{T}{12} \right) \right. \\ \left. + \left(\sum_{\mathbf{p}}' \frac{1}{\mathbf{p}^4} \right) \left(\frac{1}{4T^2} \right) + \left(\sum_{\mathbf{p}}' \frac{1}{ \mathbf{p} } \right)^2 \left(\frac{1}{4} \right) \right]$	$+ \frac{(n-1)g^4}{2}$
b2	$\frac{1}{L^{d-1}} \left[\left(-\frac{\tau^4}{3T} + \frac{T\tau^2}{6} + \frac{T^3}{720} \right) + \left(\sum_{\mathbf{p}}' \frac{1}{ \mathbf{p} ^3} \right) \left(\frac{1}{4} \right) \right]$	$+ \frac{(n-1)^2 g^4}{2TL^{d-1}}$
c0	$\frac{1}{L^{2(d-1)}} \left[\left(\frac{7\tau^4}{6T^2} + \frac{\tau^2}{12} + \frac{T^2}{1440} \right) + \left(\sum_{\mathbf{p}}' \frac{1}{\mathbf{p}^2} \right) \left(-\frac{\tau^2}{2T^2} + \frac{1}{24} \right) \right. \\ \left. + \left(\sum_{\mathbf{p}}' \frac{1}{ \mathbf{p} ^3} \right) \left(-\frac{1}{2T} \right) + \left(\sum_{\mathbf{p}}' \frac{1}{\mathbf{p}^4} \right) \left(-\frac{3}{4T^2} \right) \right]$	$+ \frac{(n-1)^2 g^4}{4}$
c1	$\frac{1}{L^{2(d-1)}} \left[\left(\frac{5\tau^4}{6T^2} - \frac{\tau^2}{12} + \frac{11T^2}{1440} \right) + \left(\sum_{\mathbf{p}}' \frac{1}{ \mathbf{p} } \right) \left(\frac{\tau^2}{T} + \frac{T}{12} \right) \right. \\ \left. + \left(\sum_{\mathbf{p}}' \frac{1}{\mathbf{p}^4} \right) \left(\frac{1}{4T^2} \right) + \left(\sum_{\mathbf{p}}' \frac{1}{ \mathbf{p} } \right)^2 \left(\frac{1}{4} \right) \right]$	$+ \frac{(n-1)g^4}{2}$
c2	$\frac{1}{L^{d-1}} \left[\left(-\frac{\tau^4}{3T} + \frac{T\tau^2}{6} + \frac{T^3}{720} \right) + \left(\sum_{\mathbf{p}}' \frac{1}{ \mathbf{p} ^3} \right) \left(\frac{1}{4} \right) \right]$	$+ \frac{(n-1)^2 g^4}{2TL^{d-1}}$
d0	$\frac{1}{L^{2(d-1)}} \left[\left(\frac{\tau^2}{T} + \frac{T}{12} \right) + \left(\sum_{\mathbf{p}}' \frac{1}{ \mathbf{p} } \right) \left(\frac{1}{2} \right) \right]^2$	$+ \frac{(n-1)^2 g^4}{4}$
d1	$\frac{1}{L^{2(d-1)}} \left(\frac{\tau^2}{T} - \tau + \frac{T}{12} \right)^2$	$+ \frac{(n-1)g^4}{2}$
e0	$\frac{1}{L^{2(d-1)}} \left[\left(\frac{\tau^2}{T} + \frac{T}{12} \right) + \left(\sum_{\mathbf{p}}' \frac{1}{ \mathbf{p} } \right) \left(\frac{1}{2} \right) \right]^2$	$- \frac{(n-1)^2 g^4}{8}$
e1	$\frac{1}{L^{2(d-1)}} \left[\left(\frac{\tau^2}{T} + \frac{T}{12} \right) + \left(\sum_{\mathbf{p}}' \frac{1}{ \mathbf{p} } \right) \left(\frac{1}{2} \right) \right]^2$	$- \frac{(n-1)g^4}{4}$
f0	$\frac{1}{L^{2(d-1)}} \left[\left(\frac{\tau^2}{T} + \frac{T}{12} \right) + \left(\sum_{\mathbf{p}}' \frac{1}{ \mathbf{p} } \right) \left(\frac{1}{2} \right) \right]^2$	$- \frac{(n-1)^2 g^4}{8}$
f1	$\frac{1}{L^{2(d-1)}} \left[\left(\frac{\tau^2}{T} + \frac{T}{12} \right) + \left(\sum_{\mathbf{p}}' \frac{1}{ \mathbf{p} } \right) \left(\frac{1}{2} \right) \right]^2$	$- \frac{(n-1)g^4}{4}$